

1 **Supplemental Material**

2
3
4
5
6 **Title: Endothelium-targeted deletion of microRNA-15a/16-1 promotes post-**
7 **stroke angiogenesis and improves long-term neurological recovery**

8
9 **Authors:**

10 Ping Sun¹, Kai Zhang¹, Sulaiman H. Hassan¹, Xuejing Zhang¹, Xuelian Tang¹, Hongjian Pu¹, R.
11 Anne Stetler¹, Jun Chen^{1,2*}, Ke-Jie Yin^{1,2*}

12
13 **Affiliations:**

14 ¹Pittsburgh Institute of Brain Disorders and Recovery, Department of Neurology, University of
15 Pittsburgh School of Medicine, Pittsburgh, PA 15213

16 ²Geriatric Research, Education and Clinical Center, Veterans Affairs Pittsburgh Healthcare
17 System, Pittsburgh, PA 15261

18
19 ***Corresponding Author:**

20 Ke-Jie Yin, Pittsburgh Institute of Brain Disorders & Recovery and Department of Neurology,
21 University of Pittsburgh School of Medicine. 200 Lothrop Street, BST S514, Pittsburgh, PA
22 15213. USA. Email: yink2@upmc.edu

23 Jun Chen, Pittsburgh Institute of Brain Disorders & Recovery and Department of Neurology,
24 University of Pittsburgh School of Medicine. 3500 Terrace Street, BST S507, Pittsburgh, PA
25 15213. USA. Email: chenj2@upmc.edu

26
27 **This PDF file includes:**

28
29 Expanded Materials & Methods

30 Online Figures I - XIX

31 Online Table I - II

33 **Supplemental Methods**

34 **Methods to prevent bias and exclusion criteria**

35 Experimental procedures were performed following criteria derived from the Stroke Therapy Academic
36 Industry Roundtable (STAIR) guidelines⁴⁷. Briefly, animals were randomly assigned with a lottery-
37 drawing box to different experimental groups, including sham or Middle Cerebral Artery Occlusion
38 (MCAO) operation, neurobehavioral evaluation, histological assessments, etc. Surgical operations and
39 outcome assessments were performed by investigators blinded to mouse genotype and experimental group
40 assignments. Although we recognized this study should be extended to female mice, only male mice were
41 included because stroke occurrence and severity can be affected by sex differences⁴⁸⁻⁵⁰, and young female
42 mice can potentially benefit from the neuroprotective and anti-inflammatory properties of estrogen^{51, 52}.
43 All mice were housed in a room where lighting was controlled (12 h on, and 12 h off) and room
44 temperature was kept around 22°C. Mice were given a standard diet and water *ad libitum*. All mice
45 subjected to MCAO received neurological deficits test at 24h after MCAO in a blinded manner. Animal
46 that showed one or more the following signs were excluded: (1) mouse receiving a neurological score less
47 than 1 (0, no visible neurological deficits; 1, forelimb flexion), (2) mouse did not show a >75% CBF
48 reduction or a <60% CBF reperfusion over baseline levels during MCAO surgery, (3) unsuccessful stroke
49 based on immuno-histological evaluation, (4) mouse did not ambulate, or swim during water-maze test,
50 (5) mouse that had greater than 20% weight loss, or were moribund and unable to attend normal
51 physiological needs such as eating, drinking, and grooming, which were euthanized, (6) animal death
52 prior to behavioral test or sample collection (see detailed information of excluded mice in **Online Figure**
53 **VB**).

54 **Choice of Sample Size**

55 Mouse numbers required for the *in vivo* studies were determined by a power analysis based on our
56 preliminary results and previous experiences with murine MCAO model in the Pittsburgh Institute of
57 Brain Disorders and Recovery. For example, to detect a 30% decrease in infarct volume or neurological
58 deficits with 80% power at an α value of 0.05 (two-tailed T-test), ~6–8 mice were needed per group; for
59 immunohistochemistry, qPCR, and western blotting, ~4–5 samples were required to detect a 30% change
60 after MCAO with 80% power ($\beta = 0.8$, $\alpha = 0.05$)^{53, 54}. However, more mice were needed to ensure
61 adequate experimental numbers after consideration of sample loss (animal mortality, exclusion of
62 animals) during these complex *in vivo* experiments to achieve statistical significance among the treatment
63 groups.

64 **Mouse model of transient focal cerebral ischemia**

65 Focal cerebral ischemia was induced by transient Middle Cerebral Artery Occlusion (MCAO)⁵⁵⁻⁵⁷.
66 Briefly, male mice (8-10 weeks, 23-26 g) were anesthetized with isoflurane (3% for induction, 1.5% for
67 maintenance) in mixed O₂ and N₂O (30%:67%). After a midline skin incision, the common carotid artery
68 was exposed, and then its branches were electro-coagulated. A 1.3-cm length of a 7-0 rounded tip nylon
69 suture was gently advanced from the external carotid artery to the internal carotid artery and further to the
70 origin of the middle cerebral artery (MCA) until regional cerebral blood flow (CBF) was reduced to less
71 than 25% of baseline. After 60 minutes of MCA occlusion, blood flow was restored by removing the

72 suture. After induction of MCAO, the mice were allowed to recover for 1 to 28 d. In sham-operated mice,
 73 the same surgical procedure was performed but without occlusion of the middle cerebral artery. Body
 74 temperature was measured with a rectal thermometer was maintained at $37.0 \pm 0.5^\circ\text{C}$ by a temperature-
 75 controlled heating pad during the ischemic period. Regional CBF was measured using a laser speckle
 76 imager (Perimed PeriCam PSI HR, Stockholm, Sweden) at 15 min before MCAO surgery, 15 min during
 77 MCAO period, and 15 min after the onset of reperfusion. Following MCAO surgery, the analgesic
 78 ketoprofen (3mg/kg) was injected intramuscularly for up to 3 days. Animals that did not show more than
 79 75% CBF reduction or a less than 60% CBF reperfusion over baseline levels or died after ischemia
 80 induction (~10% of stroke animals) were excluded from further experimentation. Physiological
 81 parameters exhibited no difference between EC-miR-15a/16-1 cKO and WT mice during the surgery, and
 82 regional CBF did not differ either (**Online Figure VI**).

83 **Isolation of cerebral microvessels**

84 Cerebral microvessels from the brain were isolated for determining the expression of microRNAs and
 85 angiogenic genes, as previously described⁵⁸⁻⁶¹ with modification. Briefly, mice were sacrificed by deeply
 86 anesthetized and transcardially perfused with cold 0.9% NaCl. The brain was immediately removed from
 87 the skull and immersed in ice-cold PBS. Brainstem, meninges and pia vessels were quickly removed, and
 88 the brain was cut into 1mm block and transfer to a 15 mL Dounce Tissue Grinder Tube (Kimble Chase,
 89 Cat # 885303-0015) with 5mL $\frac{1}{2}$ TE (0.25% Trypsin-EDTA and an equal amount of DMEM (Invitrogen,
 90 Cat #11966). The brain was homogenized by 5 strokes with a small clearance pestle. The homogenate
 91 was mixed with another 5 mL of $\frac{1}{2}$ TE and incubate at 37°C for 1 h with occasional agitation. After
 92 triturating 10-20 times with a 5 mL pipette, the creamy texture was centrifuged at 500g for 10 min at
 93 room temperature (RT). The pellet was collected and dissolved in 8 mL HBSS (Invitrogen, Cat #14170)
 94 by mixing twice with a 5 mL pipette, and the homogenate was suspended in 11 mL HBSS dissolved 25%
 95 BSA by gently triturate 5 times with a 10 mL pipette. The homogenate was centrifuged at 3,000g for 15
 96 min at 4°C to separate the lipid and the capillary fraction. The pellet was collected and rinsed with 20 mL
 97 PBS once followed by another centrifuge at 1,800g for 10 min. The pellet was rinsed with 1mL PBS,
 98 transferred to a 1.5 mL tube and centrifuged at 16,000g for 1 min. The final microvessel pellet was stored
 99 at -80°C until use.

100 **TaqMan® miRNA assay to quantify miRNA levels**

101 MiR-15a, miR-16-1, and miR-497 levels were measured as previously described^{55, 61, 62}. Briefly, total
 102 RNA was isolated from isolated mouse cerebral microvessels, cultured primary mouse brain
 103 microvascular endothelial cells (mBMECs) or primary human brain microvascular endothelial cells
 104 (hBMECs) by using a miRNeasy Mini Kit (Qiagen, Valencia, CA). Reverse transcription was performed
 105 using the TaqMan MiRNA Reverse Transcription Kit (Applied Biosystems, Foster City, CA). Polymerase
 106 chain reaction (PCR) reactions were then conducted using the TaqMan® miRNA assay Kit (Applied
 107 Biosystems). The PCR cycle conditions were shown as follows,

Stage	Temperature and time		
Enzyme Activation	95°C	10 minutes	Hold
Denaturation	95°C	15 seconds	40 cycles
Annealing/Extension	60°C	60 seconds	

108 The relative microRNA levels were calculated by the $2^{-\Delta\Delta C_t}$ method and normalized to endogenous
109 snoRNA 202 for mouse tissue or cell culture samples, or RNU48 for human cell culture samples.
110 Exosomes were extracted from the cell culture medium by Total Exosome Isolation Kit (Invitrogen,
111 Vilnius, Lithuania) for the measurement of exosomal miR-15a expression. Small RNAs were further
112 enriched by Total Exosome RNA and Protein Isolation Kit (Invitrogen, Vilnius, Lithuania) according to
113 the manufacture's protocols. Reverse transcription and TaqMan® miRNA assay were conducted as
114 described above. The relative microRNA levels were normalized to U6 snRNA for exosomal miRNA
115 expressions⁶³.

116 **Neurobehavioral tests**

117 Neurobehavioral tests were carried out before and up to 28 d after MCAO (**Online Figure III**).
118 Sensorimotor deficits were evaluated by the foot fault test, rota-rod test, and adhesive removal test. Long-
119 term cognitive deficits were evaluated by the Morris water maze test as described previously^{53, 55-57, 64}.

120 **Foot fault test.** The foot fault test was performed to assess the locomotor function for mice after stroke.
121 Mice were allowed to move on a metal grid surface by gripping the wire with paws and were tested for
122 three trials lasting 2 min each. A foot fault was counted when the forepaw fell or slipped between the
123 wires. Data were expressed as the percentage of error steps to the total moving steps of the contralateral
124 forepaw.

125 **Rota-rod test.** Mice were placed on a rotating drum (model 47650, Ugo Basile) with speeds accelerating
126 from 5 to 40 rpm within 5 min. The time was recorded when mice fell off the drum (time on rod). Three
127 trials per day were performed for 3 consecutive days before surgery and 4 trials per day were performed 3
128 d to 28 d after MCAO. The average staying time on rod of three trials 1 d before surgery was used as the
129 pre-surgery baseline value. After surgery, the mean value of trials 2-4 was used as the time on rod of the
130 tested day.

131 **Adhesive removal test.** A piece of adhesive tape dots (3mm x 3mm) was used to cover the palmar surface
132 of the contralateral forepaw. The time to contact (time to touch) and completely remove the tape (time to
133 remove) from the forepaw was recorded, respectively. Three trials daily were performed for each animal
134 from 3 d before surgery until selected time points after surgery. Mean value of three trials 1 d before
135 surgery was used as the pre-surgery baseline value.

136 **Morris water maze test.** The Morris water maze test was carried out to test 22-27 d after MCAO to
137 evaluate the long-term cognitive functions. Briefly, a circular platform (11 cm \varnothing) was submerged in one
138 quadrant of the circular pool (109 cm \varnothing) of opaque water. To examine the spatial learning ability, each
139 mouse was placed into the pool from one of the three different start points (3 trials) and allowed to swim
140 for 60 s to locate the hidden platform. The time when the mouse found the hidden platform (Escape
141 latency) was recorded for each trial. When each trial ended, the mouse was allowed to stay on the
142 platform for 20 s to help it remember the external spatial cues displayed around the room. Mice were
143 trained for three consecutive days before, and 22-26 d after MCAO (three trials per day). To evaluate
144 spatial memory, a single 60 s probe trial was performed at 27 d after MCAO when the platform was
145 removed. An investigator recorded the time that each mouse spent in the target quadrant where the
146 platform had previously been placed. Data are expressed as the percentage of the total testing time of 60 s
147 (Duration in goal quadrant).

148 **Immunohistochemistry and image analysis**

149 At multiple reperfusion time points after tMCAO (**Online Figure III**), experimental mice were deeply
150 anesthetized and transcardially perfused with 0.9% NaCl followed by 4% paraformaldehyde in PBS.
151 Brains or hindlimb gastrocnemius muscles were collected and cryoprotected in 30% sucrose in PBS for 2
152 days, and serial coronal brain or hindlimb gastrocnemius muscle sections (25- μ M thick) were prepared on
153 a microtome (HM450, Thermo Scientific). Tissue sections were transferred to cryoprotectant and stored
154 at -20°C for future tests or subjected to immunofluorescence staining as described^{54, 57, 65} with
155 modifications. After a series of washes with PBS, free-floating sections were incubated with 1% PBST
156 (1% Triton X-100 in PBS) for 20 min, followed by blocking with 5% normal donkey serum for 1 h. After
157 another series of washing with 0.3% PBST, sections were incubated overnight at 4°C with rat anti-mouse
158 CD31 (1:200, BD Pharmingen) or rabbit anti-mouse microtubule-associated protein 2 (MAP2, 1:500,
159 EMD Millipore). After a series of washes, sections were then incubated with Alexa Fluor 488 conjugated
160 donkey anti-rat (1:400, Jackson ImmunoResearch Laboratories) or donkey anti-rabbit (1:1000, Jackson
161 ImmunoResearch Laboratories) secondary antibodies, respectively. For CD31 immunofluorescent
162 staining, immunofluorescence images were captured with an Olympus Fluoview FV1000 confocal
163 microscope with FV10-ASW 2.0 software (Olympus America, Center Valley, PA). The regions of
164 interest (ROIs) were scanned at 1024 x 1024 pixels format in the x-y direction, and 1- μ M step-size optical
165 sections along the z-axis were acquired with an x 20 objective lens. Three-dimensional (3D)
166 reconstruction was performed using Adobe Photoshop CC 2018 software to quantify the vascular density,
167 the vascular surface area (mm^2), vascular length (mm), branch points and capillary number per volume of
168 tissue (mm^3) in a blinded manner. Alternatively, the imaging processing software Imaris (Bitplane,
169 Belfast, United Kingdom) was used to reconstruct 3D images of CD31 and BrdU double-labeled
170 immunostaining, as described previously⁶⁵. For MAP-2 immunofluorescent staining, images were
171 captured with an inverted Nikon Diaphot-300 fluorescence microscope equipped with a SPOT RT slider
172 camera and Meta Series Software 5.0 (Molecular Devices, Sunnyvale, CA).

173 Tomato lectin was used to identify functional vessels in the brain as described previously⁶⁶. Briefly, mice
174 were anesthetized and transcardially perfused with biotin-conjugated tomato lectin (Vector Labs,
175 Burlingame, USA) at a dose of 10 mg/kg body weight 5 min before euthanasia. Then, the mouse was
176 perfused with 0.9% NaCl followed by 4% paraformaldehyde in PBS. Coronal brain sections were
177 prepared as described above. After a series of washes with PBS, free-floating sections were incubated
178 with 1% PBST (1% Triton X-100 in PBS) for 20 min, followed by blocking with 5% normal donkey
179 serum for 1 h. After another series of washing with 0.3% PBST, brain sections were incubated with Alexa
180 Fluor® 488 streptavidin (1: 1000, Jackson ImmunoResearch Laboratories) at RT in the dark for 1 h.
181 Images were captured and analyzed in the same methods as CD31 described above.

182 Brain infarct volume or atrophy was measured on six equally spaced MAP2-stained sections
183 encompassing the MCA territory using NIH ImageJ software. These areas were summed and multiplied
184 by the distance between sections (1 mm) to yield a leakage volume in mm^3 . The actual brain infarct
185 volumes with corrections for edema were calculated as the volume of the contralateral hemisphere minus
186 the non-infarcted volume of the ipsilateral hemisphere. Tissue atrophy was calculated as the volume of
187 the contralateral hemisphere minus the ipsilateral hemisphere.

188 **Examination of *in vivo* endothelial cell proliferation by BrdU labeling**

189 The newly proliferated cells were labeled with the S-phase marker 5-bromo-2'-deoxyuridine (BrdU,
190 Sigma Aldrich) as described^{65, 66}. Briefly, BrdU (50 mg/kg body weight) was injected intraperitoneally
191 (*i.p.*) twice per day with an interval of 6 h at 3-6 days after MCAO (**Online Figure III**). Mice were
192 sacrificed at 28 days following MCAO, and coronal brain sections were prepared as described above.
193 Sections were pretreated in 1N HCl for 1h followed by 0.1M boric acid (pH 8.5) for 10 min at RT.
194 Sections were then blocked with 5% normal donkey serum in 0.3% PBST for 1 h, followed by the
195 blocking with M.O.M kit (Vector Laboratories) for 1 h at RT, then sections were incubated with purified
196 mouse anti-BrdU antibody (1:200, BD Pharmingen) for 1 h at RT and then overnight at 4°C. After a
197 series of washes, sections were incubated with Cy3 AffiniPure Donkey Anti-Mouse IgG (1:400, Jackson
198 ImmunoResearch Laboratories) for 1 h at RT in the dark. Fluorescence images were captured as described
199 above. BrdU immunopositive cells were counted using ImageJ and calculated as the number of BrdU⁺
200 cells in the designated fields divided by the volume (mm³). Newly formed microvessels were assessed by
201 counting BrdU immunopositive cells along the microvessels in BrdU/CD31 double-immunostained
202 sections. To detect newly formed functional vessels in the penumbral area, BrdU was injected over four
203 consecutive days within the first week following reperfusion to identify newly formed cells, then tomato
204 lectin was transcidentally perfused 28 d following stroke to determine whether the newly formed cells in
205 the acute phase after stroke successfully matured into functional vessels. Newly formed functional vessels
206 were assessed by counting BrdU immunopositive signals among blood vessels in BrdU/Tomato-lectin
207 double-immunostained sections. At least 4 microscopic fields were randomly selected in the penumbral
208 areas of each section.

209 **Laser Speckle Imaging**

210 A laser speckle imager (Perimed PeriCam PSI HR, Stockholm, Sweden) was used to monitor the regional
211 cerebral blood flow (CBF) after MCAO as described previously^{54, 55, 57}. Briefly, mice were anesthetized
212 (3% for induction, 1.5% for maintenance) and the head was fixed in a head holder in a prone position. The
213 scalp was shaved, and a middle incision was made to expose the skull. The skull surface was illuminated
214 by a laser diode (785 nm) which allowed the laser to penetrate through the brain in a diffused manner.
215 Cerebral blood flow (CBF) was measured by speckle contrast, which is the ratio of the standard deviation
216 of pixel intensity to mean pixel intensity, represents the speckle visibility relative to the velocity of the
217 light-scattering particles (blood). The speckle contrast was then converted to correlation time values,
218 which are inversely proportional to mean blood flow velocity. Two-dimensional microcirculation images
219 were captured 15 min before MCAO, 15 min after the onset of MCAO, and 15 min, 24 h, 7 d, 14 d, 21 d,
220 and 28 d after the onset of reperfusion (**Online Figure III**). For each animal, five consecutive images
221 were captured at each time point. For image data analysis, two identical elliptical regions of interest
222 (ROIs) were created on ipsilateral and the contralateral hemispheres of each image. The blood flow
223 perfusion index was first determined as the ratio of ischemic to non-ischemic CBF and then further
224 normalized to the presurgical baseline to obtain the relative CBF value for each animal.

225 **Cell cultures**

226 C57BL/6 mouse primary brain microvascular endothelial cells (mBMECs) were purchased from Cell
227 Biologics, Inc. (Chicago, IL, USA). Primary mBMECs (2-9 passages) were cultured as recommended on
228 tissue culture-treated plates in complete mouse endothelial cell medium supplemented with 10% FBS and
229 supplement kit (M1168, Cell Biologics). Primary human brain microvascular endothelial cells (hBMECs)

230 were purchased from Cell Systems (ACBRI 376, Kirkland, WA, USA). Primary hBMECs were grown in
231 EGM-2 MV BulletKit medium (CC-3202, Lonza, Walkersville, MD, USA) as described previously⁵⁴.
232 Mouse brain microvascular endothelial cell line bEnd3 cells were purchased from the American Type
233 Culture Collection (ATCC, VA, USA), and were cultured in DMEM (ATCC, 30-2002) supplemented
234 with non-heat-inactivated 10% FBS. 293TN producer cells were purchased from System Biosciences
235 (SBI, CA, USA) and cultured in DMEM (Thermo Fisher Scientific, 11995) supplemented with 10% FBS
236 and 1X GlutaMAX (Thermo Fisher Scientific, 35050). All the cells were maintained at 37°C in a
237 humidified atmosphere containing 5% CO₂, and cell medium was changed every 2-3 days.

238 **OGD model**

239 Combined oxygen and glucose deprivation (OGD) and reoxygenation were performed as an in vitro
240 model of ischemic stroke as previously described⁶⁷⁻⁶⁹ with modifications. Briefly, for OGD treatment,
241 mBMECs or hBMECs (90-95% confluency) were washed and incubated with 5% CO₂-balanced N₂
242 bubbled glucose-free DMEM (Thermo-Fisher Scientific), then cells were placed in a hypoxic chamber
243 (model MIC-101, Billups-Rothenberg). The hypoxic environment was achieved by flushing the chamber
244 for 20 min with 5% CO₂-balanced N₂. The hypoxic chamber was then transferred to a 37°C incubator.
245 Control cells were maintained with normal growth medium in the 37°C incubator under normoxic
246 conditions (5% CO₂/95% air). For reoxygenation, the medium of OGD treated cells were replaced with
247 normal growth medium, cells were returned to normoxic conditions in the 37°C incubator. In exosomal
248 miR-15a measurement (**Online Figure XIX**), reoxygenation was achieved by adding 4.5g/L glucose to
249 the OGD medium after OGD 4h and returning to 37°C incubator. Normoxia was achieved by washing
250 and maintaining the cells with glucose-free DMED plus 4.5g/L glucose in the 37°C incubator under
251 normoxic conditions.

252 **Lentivirus generation for gain- or loss- of-miR-15a/16-1 function**

253 To achieve loss- or gain-of-miR-15a functions, several lentivirus vectors below were custom-made by
254 SBI company (Palo Alto, CA, USA). MiRZipTM lentivector carrying small hairpin RNAs targeting 22nt
255 of mature mmu-miR-15a sequence (miRbase Accession number MIMAT0000526) (miRZip 15a, **Online**
256 **Figure VIII B**) or corresponding scramble control (miRZip GFP, **Online Figure VIII A**) were generated.
257 In parallel, lenti miR precursor vector carrying 84 bp mouse pre-miR-15a sequence (miRbase Accession
258 number MI0000564) (Lenti miR-15a, **Online Figure VIII D**) or non-functional control (Lenti GFP,
259 **Online Figure VIII C**) were constructed as well. Then, the recombinant lentiviral vectors were
260 transfected into 293TN cells at the present of pureFection transfection reagent (SBI) and pPACKH1
261 Packaging Plasmid Mix (mixture of three plasmids: pPACKH1-GAG, pPACKH1-REV, and pVSV-G) for
262 48-72 h, medium was collected and lentiviral particles were further precipitated with PEG-it virus
263 precipitation solution (SBI) and stored at -80°C. For mBMEC, hBMEC or bEnd3 cell infection, an equal
264 amount of miRZip GFP and miRZip 15a or Lenti GFP and Lenti miR-15a were diluted in antibiotic-free
265 growth medium and incubated with 50-60% confluent cells for 48-72 h. Cells were ready for experiments
266 and images were captured under EVOSTM FL Imaging System using a green fluorescent protein (GFP)
267 filter (Life Technologies) when 70-80% cells were infected with lentiviruses that exhibited green
268 fluorescence.

269 **Capillary tube formation assay**

270 The capillary tube formation assay was performed as previously described⁷⁰⁻⁷². Briefly, a 24-well plate
271 was coated with Matrigel® Basement Membrane Matrix at 37°C for 1 h, then lentivirus infected primary
272 mBMECs were re-seeded in BD Matrigel matrix-coated 24-multiwell plates (4 x 10⁴ cells/well) in EGM-
273 2 BulleKit medium (cc-3162; Lonza) for 4-6 h. For primary hBMECs, lentivirus infected cells were re-
274 seeded in in BD Matrigel matrix-coated 24-multiwell plates (4 x 10⁴ cells/well) in EGM-2 MV BulletKit
275 medium (CC-3202, Lonza) for 18-20h, and plate was carefully washed with culture medium once to
276 remove dead cells and debris. Tubular structures were photographed under an EVOS™ XL Core Imaging
277 System (Life Technologies), and quantified by counting the number of branch points and measuring total
278 tube length with ImageJ software.

279 ***In vitro* scratch assay**

280 The *In vitro* scratch assay was carried out as previously described^{70, 73}. Briefly, primary mBMECs or
281 hBMECs were seed on a 6-well plate and infected with lentivirus for 48-72 h, and a wound was created in
282 the mBMECs or hBMECs monolayer by a pipette tip, cells were changed to fresh medium and incubated
283 at 37°C for about 24 h. Images were captured under an EVOS™ XL Core Imaging System (Life
284 Technologies) and cellular migration was determined by ImageJ software. Relative migration rate was
285 calculated as $(\text{Area}_{\text{wound at 0 h}} - \text{Area}_{\text{wound at 24 h}}) / \text{Area}_{\text{wound at 0 h}}$.

286 **BrdU cell proliferation assay**

287 A BrdU cell proliferation kit (Millipore-Sigma) was used to determine cell proliferation according to the
288 manufactory's instruction. Briefly, lentivirus infected primary mBMECs or hBMECs were seeded on a
289 96-well plate and pulsed with BrdU reagent at 37°C for 20 h. After fixing the cells for 30 min, cells were
290 incubated with mouse anti-BrdU antibody at RT for 1 h, and then cells were incubated with peroxidase
291 labeled goat anti-mouse IgG at RT for 30 min. After incubating with the substrate in the dark for 30 min,
292 the stop solution was added, and the color was spectrophotometrically quantified at 450nm in a
293 microplate reader (SpectraMax i3x, Molecular Device).

294 **Transfection of hBMECs with siRNAs**

295 Primary hBMECs were transfected with VEGFA and FGF2 siRNA (ThermoFisher Scientific) to
296 knockdown their expressions according to the manufacturer's instructions. Briefly, primary hBMECs
297 were seeded at 30% confluence without antibiotics one day before transfection. Cells were then
298 transfected with 25 nM VEGFA siRNA (Cat # 4392420, assay ID # s228861), 25 nM FGF2 siRNA (Cat
299 #4392420, assay ID # s5129), or 25 nM scrambled siRNA (Cat # 4390846, ThermoFisher Scientific), in
300 the presence of lipofectamine RNAiMAX (Cat # 13778-150, Invitrogen) and Opti-MEM I reduced Serum
301 Medium (Cat # 11058-021, ThermoFisher Scientific). Cells were incubated at 37°C incubator for 24
302 hours and ready for the next experiment.

303 **Quantitative real-time PCR**

304 As previously described, total RNA was isolated from the 0.9% NaCl perfused mouse cerebral cortex,
305 primary mBMEC, or primary hBMEC cultures by using TRIzol (Invitrogen) or RNeasy Mini Kit
306 (Qiagen), respectively^{56, 57}. Quantitative real-time reverse transcriptase PCR was performed with a Bio-
307 Rad CFX connect thermocycler, iScript cDNA synthesis kit (ThermoFisher Scientific), and iTaq

308 Universal SYBR Green Supermix (Bio-Rad). Specific primers used for the PCR reaction are presented in
309 detail in **Online Table I**. The PCR cycle conditions were shown as follows,

Stage	Temperature and time		
Enzyme Activation	95°C	3 minutes	Hold
Denaturation	95°C	10 seconds	40 cycles
Annealing	59°C	20 seconds	
Extension	72°C	30 seconds	

310 The relative mRNA expression was calculated by the $2^{-\Delta\Delta C_t}$ method and normalized to mouse or human
311 cyclophilin RNA levels. PCR experiments were repeated at least 3 times, each using separate brain cortex
312 or cell culture samples.

313 **Western Blot**

314 Samples from the 0.9% NaCl perfused mouse cerebral cortex, primary mBMEC or hBMEC cultures were
315 homogenized in 1x RIPA buffer (Thermo Scientific) containing Mini Protease Inhibitor Cocktail
316 (cOmplete™, Sigma). Protein concentrations were measured using the Bio-Rad Protein Assay (Bradford,
317 Bio-Rad). As previously described⁶⁷⁻⁶⁹, equal amounts of protein were loaded into 4-15% precast gels
318 (Bio-Rad) and transferred to polyvinylidene difluoride (PVDF, Bio-Rad) membranes. Membranes were
319 blocked for 1 h with TBS/0.1%-Tween buffer plus 5% (w/v) non-fat dried milk and incubated overnight
320 at 4°C with primary antibodies diluted in 5% BSA (dissolved in TBS/0.1%-Tween). Membranes were
321 then incubated with secondary antibodies diluted in 5% BSA for 1 h and developed using a Pierce® ECL
322 Western blotting detection kit (Thermo Scientific) and Amersham High-Performance Chemiluminescence
323 Films (GE Healthcare). The primary antibodies used are listed in **Online Table II**; secondary HRP
324 (horseradish peroxidase)-conjugated antibodies used were anti-rabbit IgG (1: 2000) (Cell Signaling;
325 Beverly, MA, USA), and anti-mouse IgG (1: 2000) (Cell Signaling). Secondary antibody controls were
326 performed by incubating the membranes only with secondary antibodies, which yielded no bands. The
327 ImageJ software was used to quantify Western blot signals.

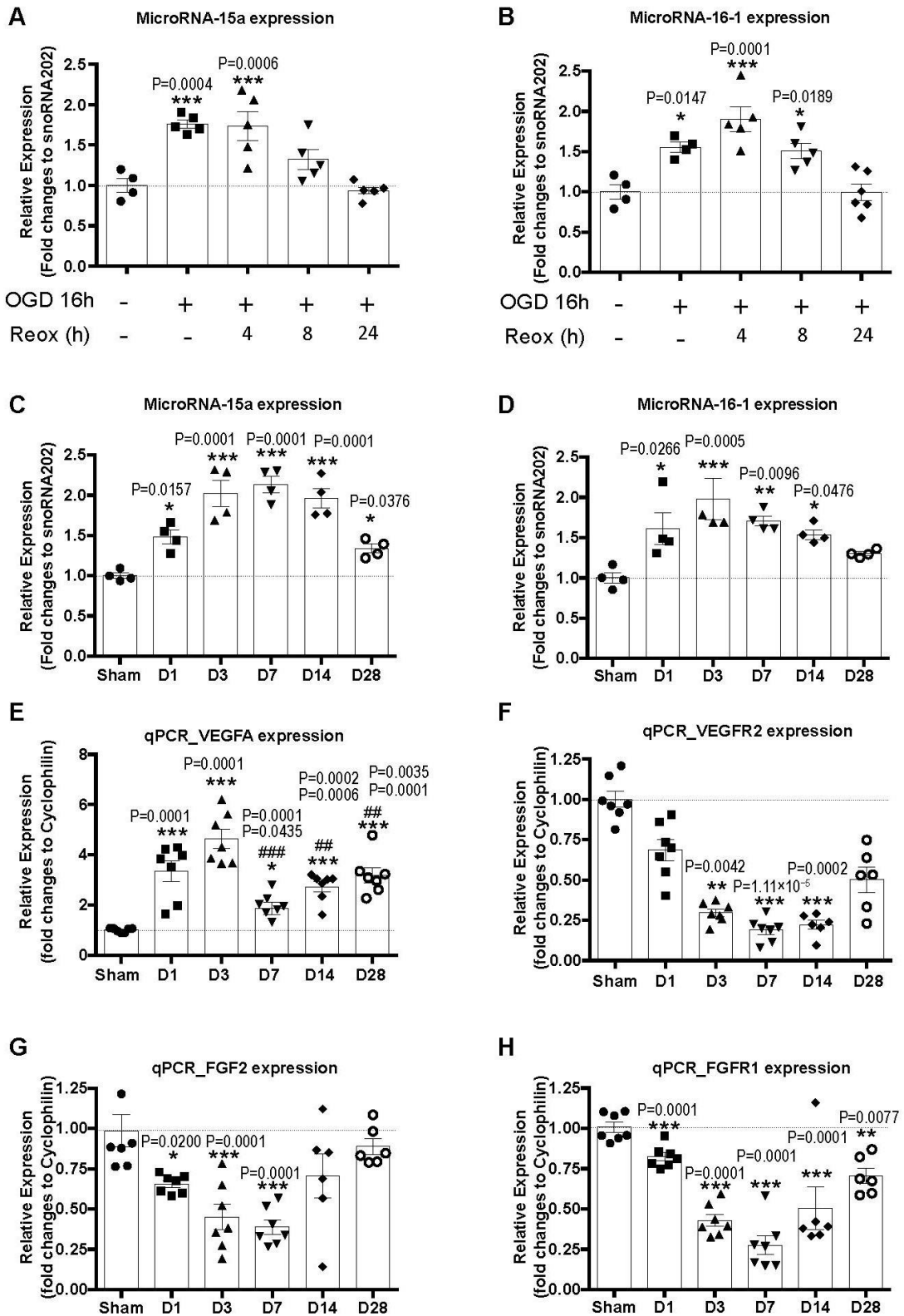
328 **Dual-luciferase reporter assay**

329 To explore the regulatory mechanism of the miR-15a/16-1 cluster on pro-angiogenic factors, a dual-
330 luciferase reporter assay was performed as previously described⁷⁰. Briefly, a miTarget microRNA 3'-UTR
331 luciferase vector (pEZX-MT01), in which a 1862-bp fragment of the 3'-UTR of the mouse VEGFA
332 mRNA, a 1608-bp fragment of the 3'-UTR of the mouse VEGFR2 mRNA, a 5666-bp fragment of the 3'-
333 UTR of the mouse FGF2 mRNA or a 1804-bp fragment of the 3'-UTR of the mouse FGFR1 mRNA
334 containing the putative miR-15a/16-1 binding sequence, was directly purchased from GeneCopoeia
335 (Rockville, MD). Mutant 3'-UTR fragment of the mouse VEGFA, VEGFR2, FGF2 and FGFR1 with
336 deletion of the predicted miR-15a/16-1 binding sequence were generated by using overlapping PCR
337 followed by DNA ligation and transformation in E.Coli bacteria on Kanamycin selection Luria Broth
338 (LB) agar plate. The primers and their sequences were listed in **Online Table I**. The sequences of the
339 plasmid DNAs extracted from the bacterial colonies were further validated by DNA sequencing. Mouse
340 brain microvascular endothelial cell line bEnd3 cells were plated on 24-well plates. At the following day,
341 when cells reached 50-60% confluency, cells were infected with various lentiviruses in order to achieve
342 loss- or gain-of miR-15a/16-1 functions. Seventy-two hours following lentiviruses infection, cells were

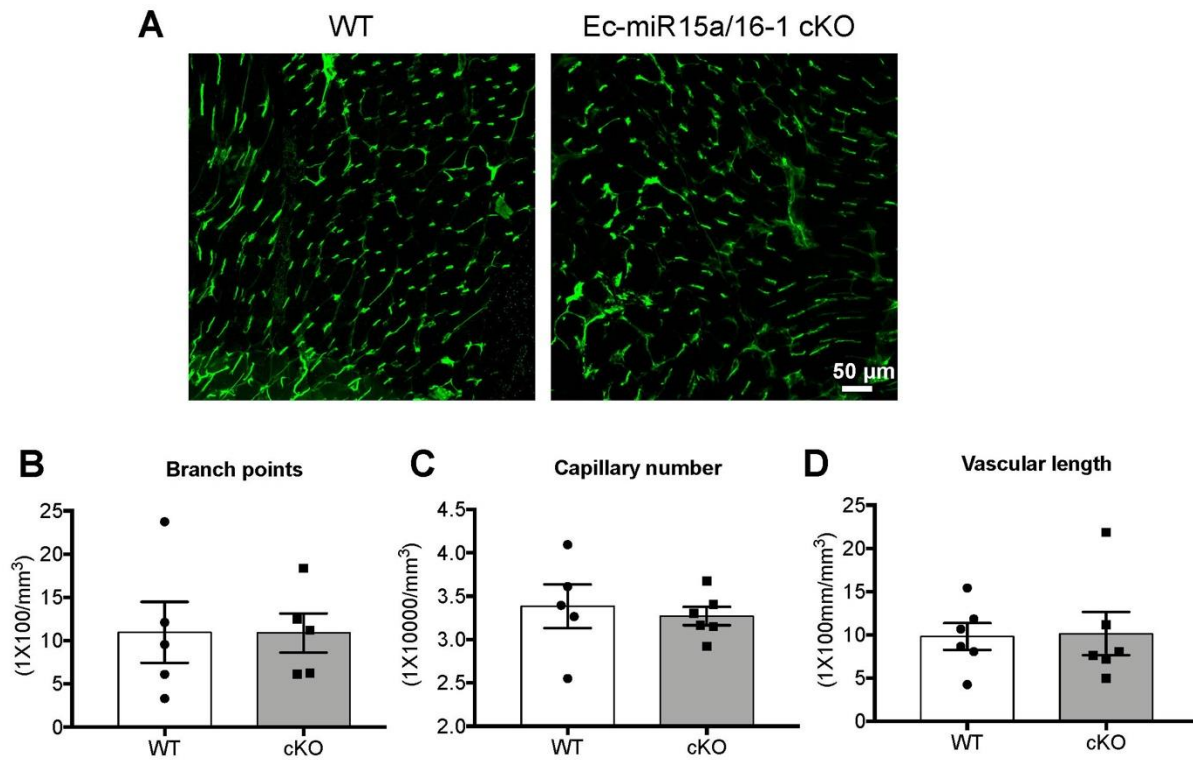
343 co-transfected with mVEGFA, mVEGFR2, mFGF2 or mFGFR1 3'-UTR luciferase reporter constructs
344 and their corresponding controls with deletions of putative miR-15a/16-1 binding sites, along with
345 Lipofectamine 2000 (Invitrogen) for 6 h. *Firefly* and *Renilla* luciferase activity were determined 48 h after
346 transfection using Dual-Luciferase assay kit (Promega) with a microplate reader (SpectraMax i3x,
347 Molecular Device). Individual relative luciferase activity was normalized to the corresponding *Renilla*-
348 luciferase activity.

349 **Statistical analyses**

350 Data are presented as mean \pm SEM. The Gaussian distribution of each variable was checked using the
351 Shapiro-Wilk test if $N < 30$ and Kolmogorov-Smirnov test if $N \geq 30$. Non-normally distributed data were
352 analyzed by nonparametric tests: Mann-Whitney test for two groups, and Kruskal-Wallis test followed by
353 Dunn's post hoc analysis for three or more groups. Normally distributed data were analyzed by using
354 parametric tests: two-tailed Student's t-test between two groups, and one-way ANOVA followed by
355 Tukey's (compares every mean with every other mean) or Dunnett's (compares every mean to a control
356 mean) multiple comparison tests for three or more groups. Experiments consisting of two categorically
357 independent variables and one dependent variable were analyzed by two-way ANOVA followed by
358 Bonferroni's multiple comparison tests. Multiple comparisons among three or more groups were
359 corrected using the Tukey's, Dunnett's, Dunn's and Bonferroni's testing through controlling the Type I
360 error for the family of comparisons. Statistical analyses for survival rate were performed by Log-rank
361 (Mantel-Cox) test and Gehan-Breslow-Wilcoxon test. A $p < 0.05$ was considered to be statistically
362 significant. All of these statistical analyses and graphic representations were obtained by using the
363 GraphPad Prism 7.0 software.
364



367 **Online Figure I. The expressions of miR-15a/16-1 cluster and pro-angiogenic factors are altered**
368 **after cerebral ischemia.** Primary mBMECs were subjected to OGD 16h or/and reoxygenation (Reox) 4h,
369 8h and 24h. Non-OGD treated cells in normoxic conditions served as controls. qPCR data showed that the
370 expression of miR-15a (**A**) and miR-16-1 (**B**) are significantly increased in primary mBMECs subjected
371 to OGD 16h or/and Reox 4h and 8h. In addition, Male C57BL/6J mice were subjected to 1h MCAO
372 followed by 1-28 d reperfusion. Brains were harvested and microvessels were extracted from the
373 ipsilateral hemisphere of the brain. Compared to sham group, qPCR data indicated that the relative
374 expression of miR-15a (**C**) and miR-16-1 (**D**) are significantly elevated in microvessels isolated from the
375 ipsilateral brains of mice subjected to 1h MCAO followed by 1-28 d reperfusion (D1-D28). The relative
376 microRNA expressions were normalized to snoRNA202 levels. Moreover, for analyses of angiogenic
377 factors, qPCR data showed significantly up-regulated mRNA expression profile for VEGFA (**E**) and
378 down-regulated expression profile for VEGFR2 (**F**), FGF2 (**G**) and FGFR1 (**H**) in microvessels isolated
379 from ipsilateral brains of mice subjected to 1h MCAO followed by 1-28 d reperfusion in comparison with
380 sham group. The mRNA expressions were normalized to cyclophilin levels. Data are expressed as mean \pm
381 SEM, n = 4-6/group for all qPCR assays. * $p < 0.05$, ** $p < 0.01$, *** $p < 0.001$ versus non-OGD treated cells
382 or sham group; ## $p < 0.01$, ### $p < 0.001$ versus 3 d after reperfusion in **E**; statistical analyses were
383 performed by one-way ANOVA followed by Dunnett's multiple comparison tests for **A-E**, **G** and **H**;
384 statistical analyses were performed by Kruskal-Wallis test followed by Dunn's multiple comparison tests
385 for **F**.
386



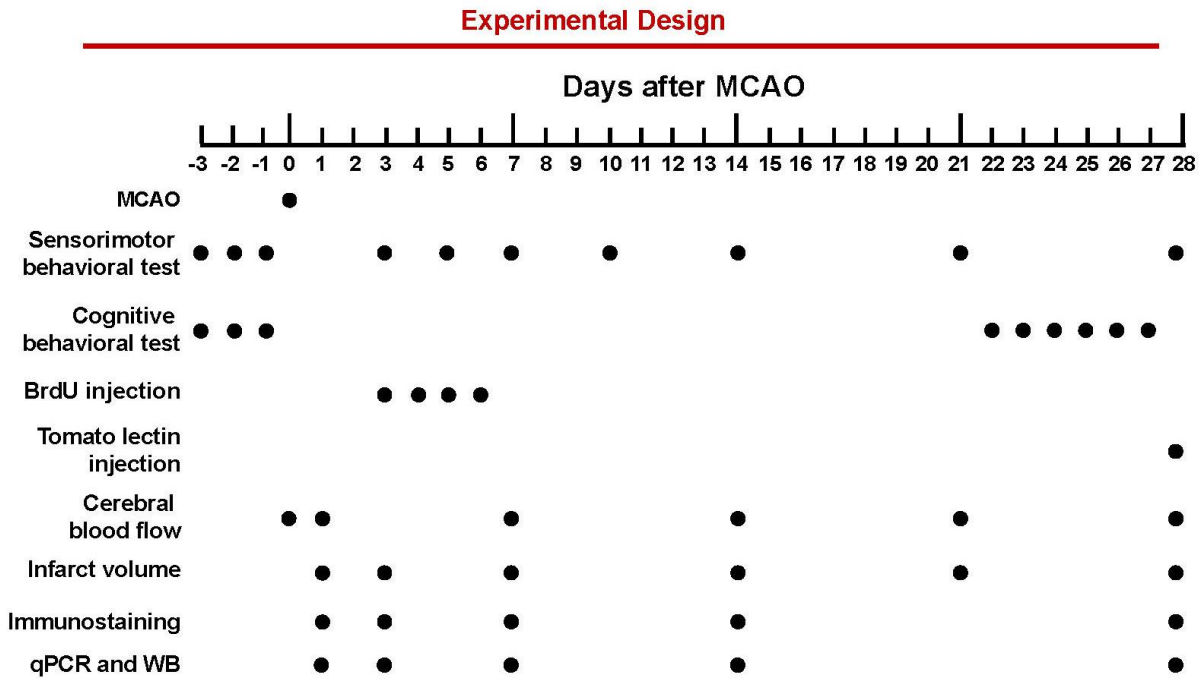
388

389 **Online Figure II. Microvasculature in hindlimb gastrocnemius muscles of WT and EC-miR-15a/16-**
 390 **1 cKO mice.** Microvasculature in hindlimb gastrocnemius muscles was examined and quantified in sham-
 391 operated WT and EC-miR-15a/16-1 cKO mice by immunostaining of CD31. **A-D**, Representative CD31
 392 fluorescent images (**A**), the quantification of branch points (**B**), capillary number (**C**) and vascular length
 393 (**D**) showing no statistically significant difference in the microvascular anatomy of hindlimb
 394 gastrocnemius muscles between WT and EC-miR-15a/16-1 cKO animals. Data are expressed as mean \pm
 395 SEM; $n = 5-6/\text{group}$; statistical analyses were performed by two-tailed Student's t-test.

396

397

398

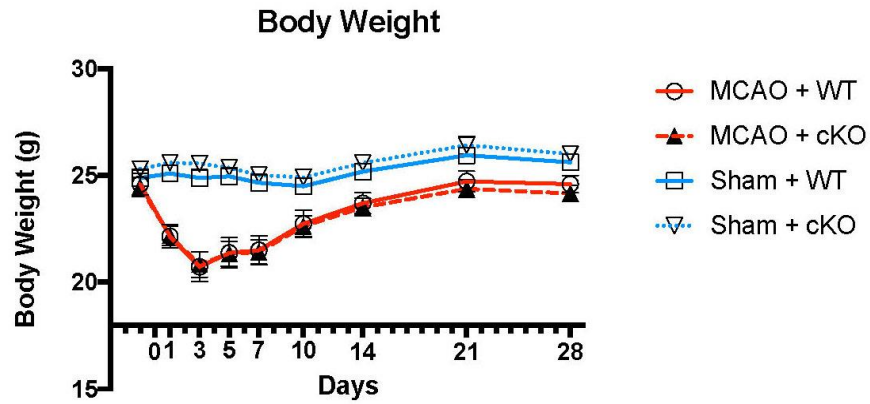


399

400 **Online Figure III. Schematic diagram of experimental design.** Mice were subjected to 1 h transient
401 middle cerebral artery occlusion (tMCAO). Neurobehavioral tests were performed up to 28 d after
402 tMCAO. To detect newly proliferated cells, BrdU was injected intraperitoneally twice per day with an
403 interval of 6 h at 3-6 d after MCAO. To examine functional blood vessels, tomato lectin was injected
404 transcidentally 5 min before euthanasia. Cerebral blood flow was monitored by laser speckle imaging at 15
405 min before MCAO, 15 min after the onset of MCAO, and 15 min, 1 d, 7 d, 14 d, 21 d, and 28 d after the
406 onset of reperfusion. Immunohistological and biochemical analysis utilized brain samples was harvested
407 at indicated time points.

408

409

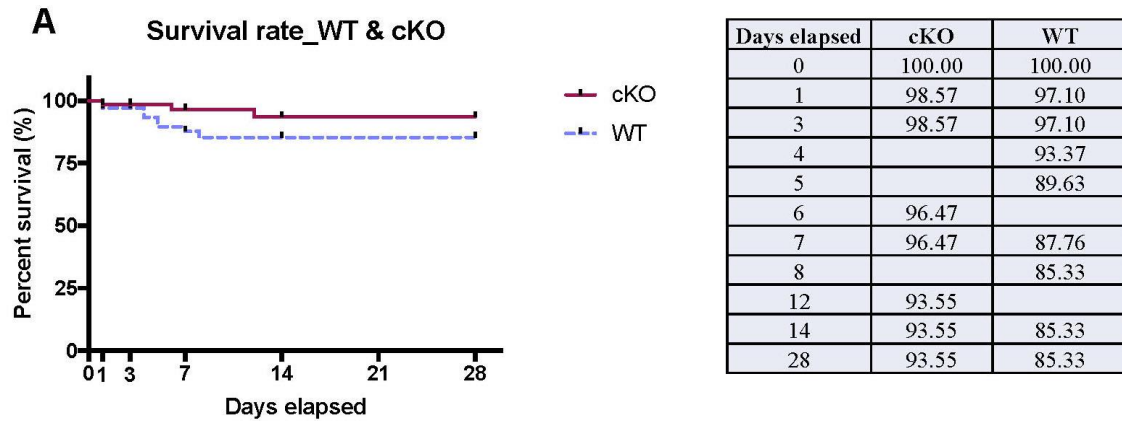


410

411

412 **Online Figure IV. Sequential tracing of body weight in WT or endothelium-targeted miR-15a/16-1**
413 **deletion mice.** Body weight of EC-miR-15a/16-1 cKO and WT mice were measured before or 1-28 d
414 after MCAO, sham treated animals were also measured at indicated time points. EC-miR-15a/16-1 cKO
415 and WT mice showed similar patterns of weight change. Data were shown as mean \pm SEM; n = 10 for
416 sham groups, n = 13-14 for MCAO groups.

417

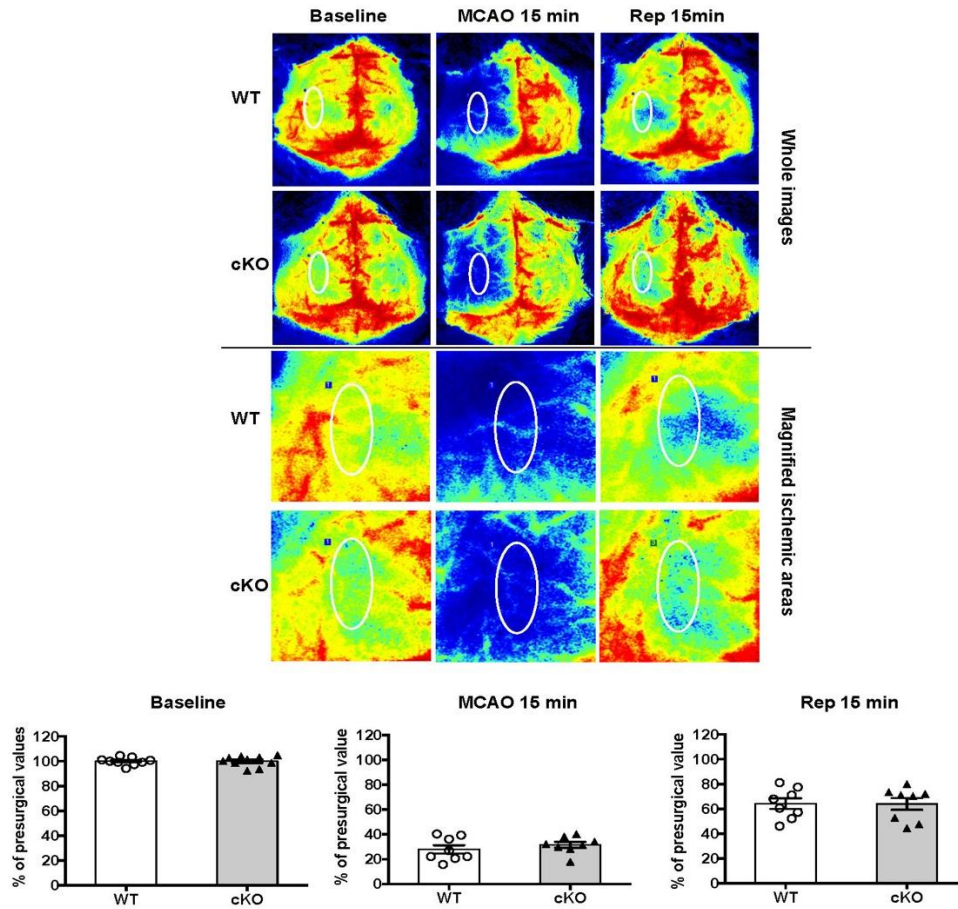


B

Studies	Excluded animal number	Experimental groups	Time points	Reasons
Neurobehavioral test	2	WT MCAO	Day 0	Death on the day of surgery
	1	WT MCAO	Day 1	Neurological score < 1
	1	WT MCAO	Day 1	Seizure and Death
	1	WT MCAO	Day 4	Death
	1	WT MCAO	Day 25	Not swim during water-maze test
	1	cKO MCAO	Day 0	Death on the day of surgery
	1	cKO MCAO	Day 1	Neurological score < 1
Cerebral blood flow (CBF) measurement	2	WT MCAO	Day 0	Death on the day of surgery
	1	cKO MCAO	Day 0	Death on the day of surgery
	1	cKO MCAO	Day 0	CBF <60% reperfusion over baseline levels after MCAO
Immunohistochemical and biochemical experiments	1	WT MCAO	Day 0	Death on the day of surgery
	1	WT MCAO	Day 4	Death
	2	WT MCAO	Day 5	Death
	1	WT MCAO	Day 7	Death
	1	WT MCAO	Day 8	Death
	3	WT MCAO	Day 14	No infarction
	1	cKO MCAO	Day 1	Death
	1	cKO MCAO	Day 5	Moribund and unable to eat and drink, euthanized
	1	cKO MCAO	Day 12	Death
	2	cKO MCAO	Day 28	No infarction

418

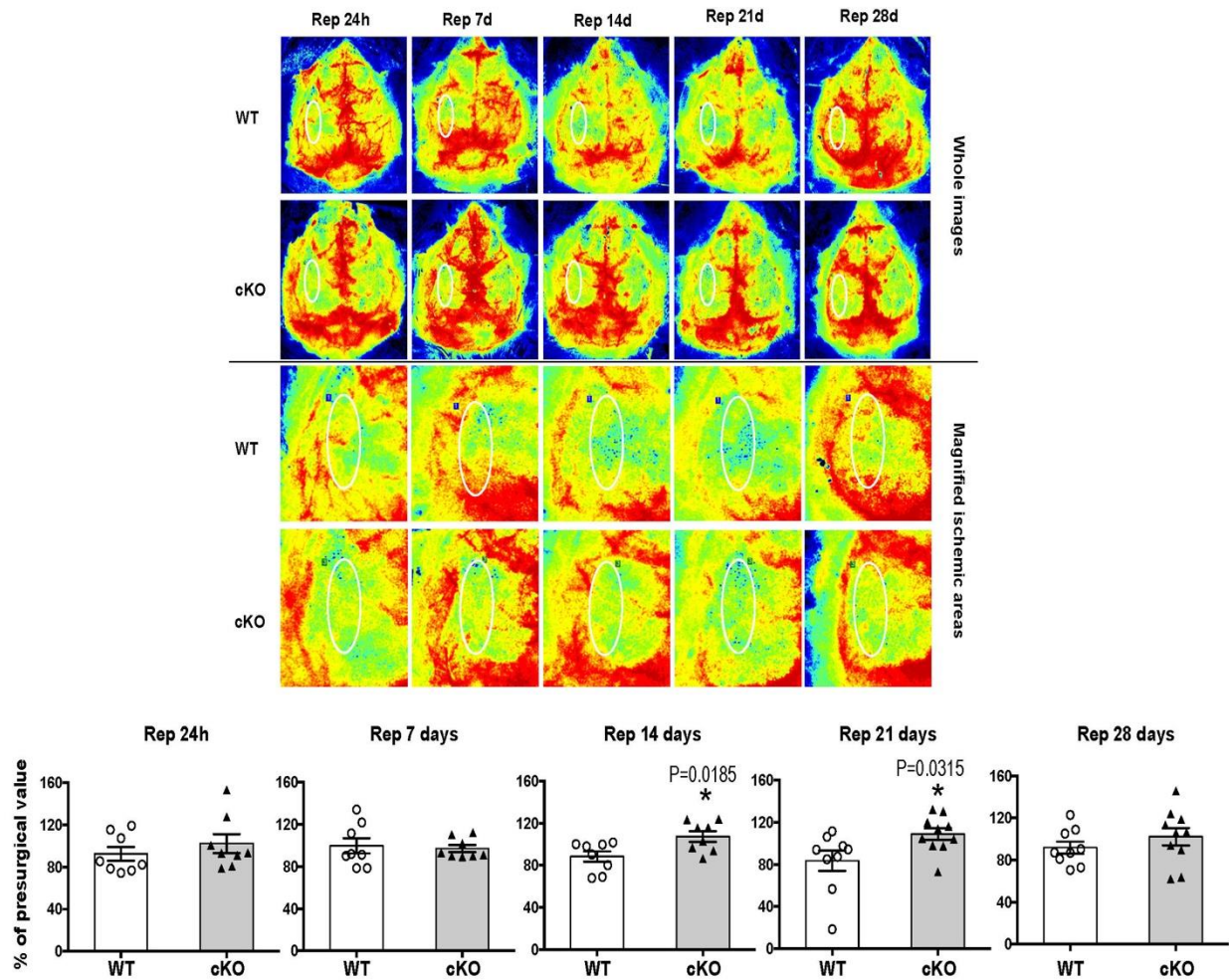
419 **Online Figure V. Sequential tracing of survival rate in WT or endothelium-targeted miR-15a/16-1**
 420 **deletion mice.** **A**, The survival curve of EC-miR-15a/16-1 cKO and WT mice after MCAO was traced
 421 and each death event was recorded immediately. No survival rate difference was found between two
 422 genotypes of mice following MCAO. n = 70 for EC-miR-15a/16-1 cKO mice and n = 69 for WT mice. **B**,
 423 All animals excluded from the analyses with respective group that fulfilled the exclusion criteria.
 424 Statistical analyses were performed by Log-rank (Mantel-Cox) test ($p = 0.1500$) and Gehan-Breslow-
 425 Wilcoxon test ($p = 0.1448$).
 426



428

429 **Online Figure VI. Effect of endothelium-targeted deletion of the miR-15a/16-1 cluster on regional**
 430 **cerebral blood flow during cerebral ischemia surgery.** Laser speckle imager was used to measure the
 431 regional CBF in EC-miR-15a/16-1 cKO and WT mice during MCAO surgery. Representative CBF
 432 images were shown at 15 min before cerebral ischemia (Baseline), 15 min after ischemia (MCAO 15 min)
 433 and 15 min after reperfusion (Rep 15 min). Two identical elliptical ROIs were selected as indicated on the
 434 ipsilateral and contralateral hemispheres. The relative CBF was first determined as the ratio of ischemic to
 435 non-ischemic values, and then normalized to the pre-MCAO baseline for each animal. Quantitative data
 436 analyses showed similar changes in regional CBF between EC-miR-15a/16-1 WT and cKO mice. Data
 437 are expressed as mean \pm SEM; n = 8-10/ group; statistical analyses were performed by two-tailed
 438 Student's t-test.

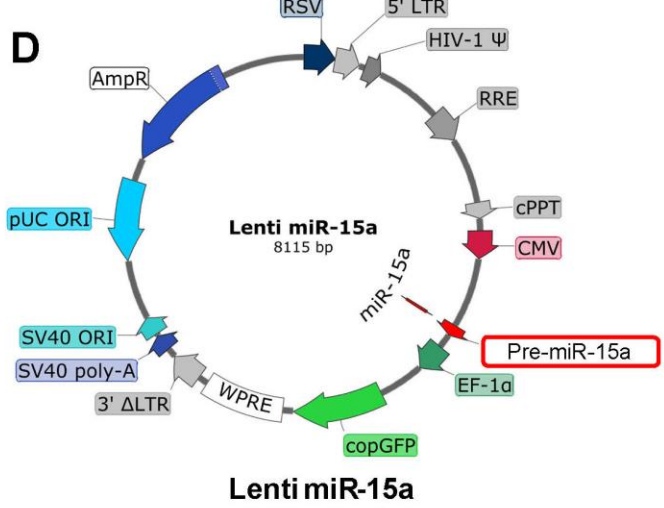
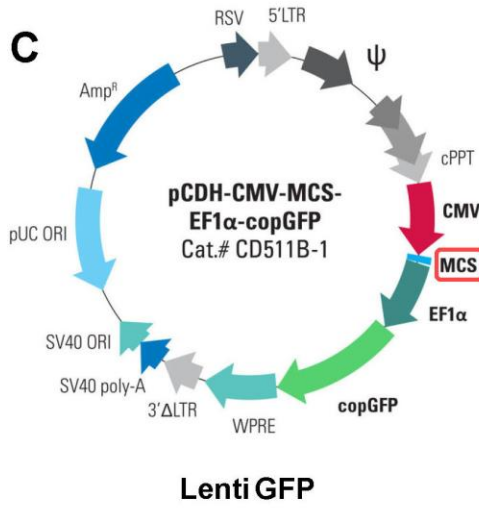
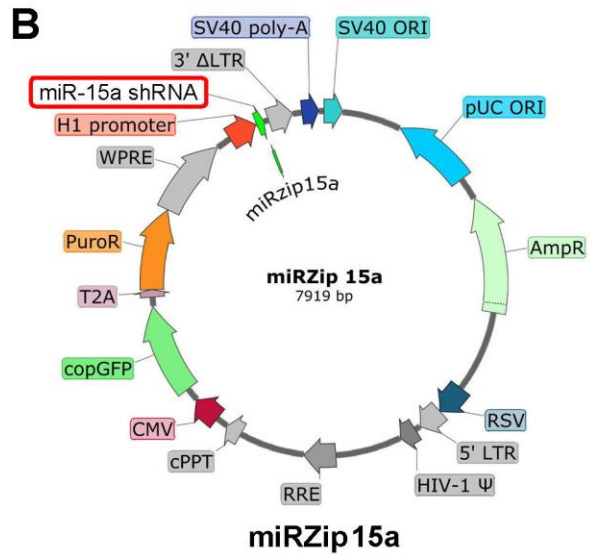
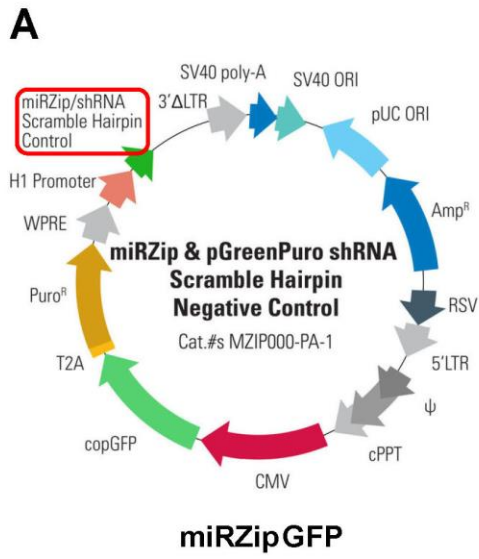
439



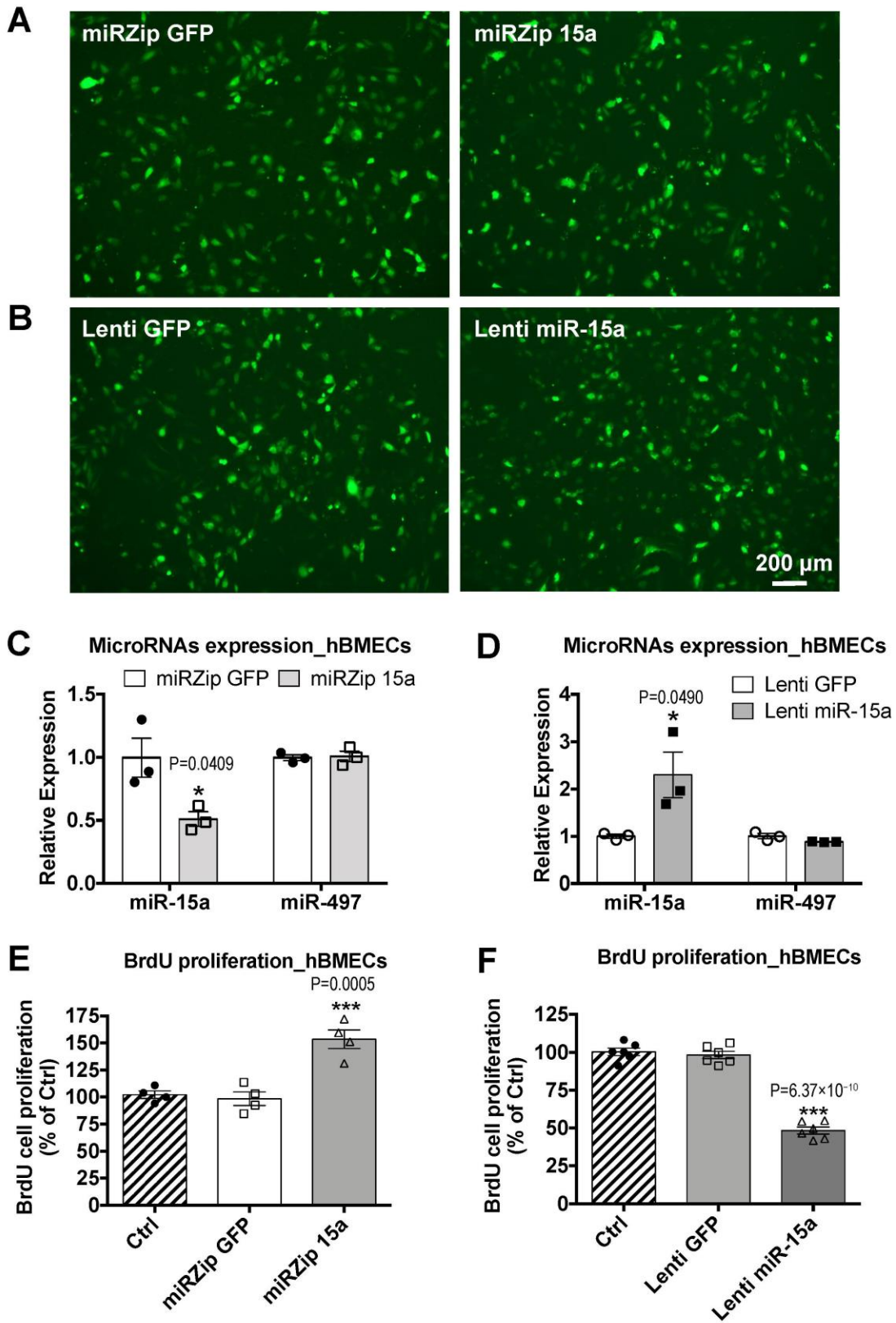
441

442 **Online Figure VII. Endothelium-targeted miR-15a/16-1 deletion improves cerebral blood flow**
 443 **recovery in mice after cerebral ischemia.** EC-miR-15a/16-1 cKO and WT mice were subjected to 1h
 444 MCAO followed by 1-28 d reperfusion. Representative CBF images were shown at 24 h, 7 d, 14 d, 21 d
 445 and 28 d after the onset of reperfusion. Two identical elliptical ROIs were selected as indicated on the
 446 ipsilateral and contralateral hemispheres. The relative CBF was first determined as the ratio of ischemic to
 447 non-ischemic values, and then normalized to the pre-MCAO baseline for each animal. Quantitative data
 448 analyses demonstrated that the relative CBF value in EC-miR-15a/16-1 cKO mice exhibited a significant
 449 increase at 14 d and 21 d of reperfusion after MCAO. Data are expressed as mean \pm SEM; n = 8 for each
 450 group; * $p < 0.05$ versus WT group; statistical analyses were performed by two-tailed Student's t-test.

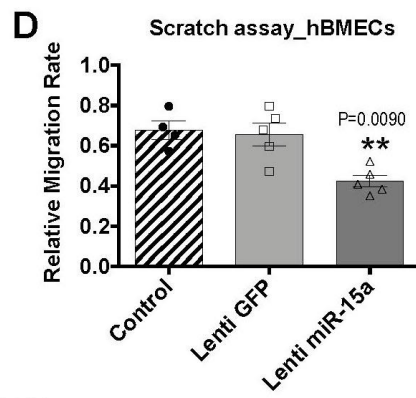
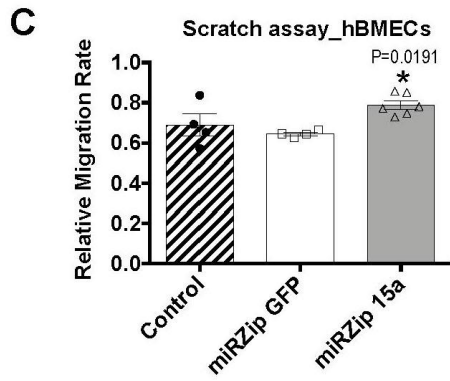
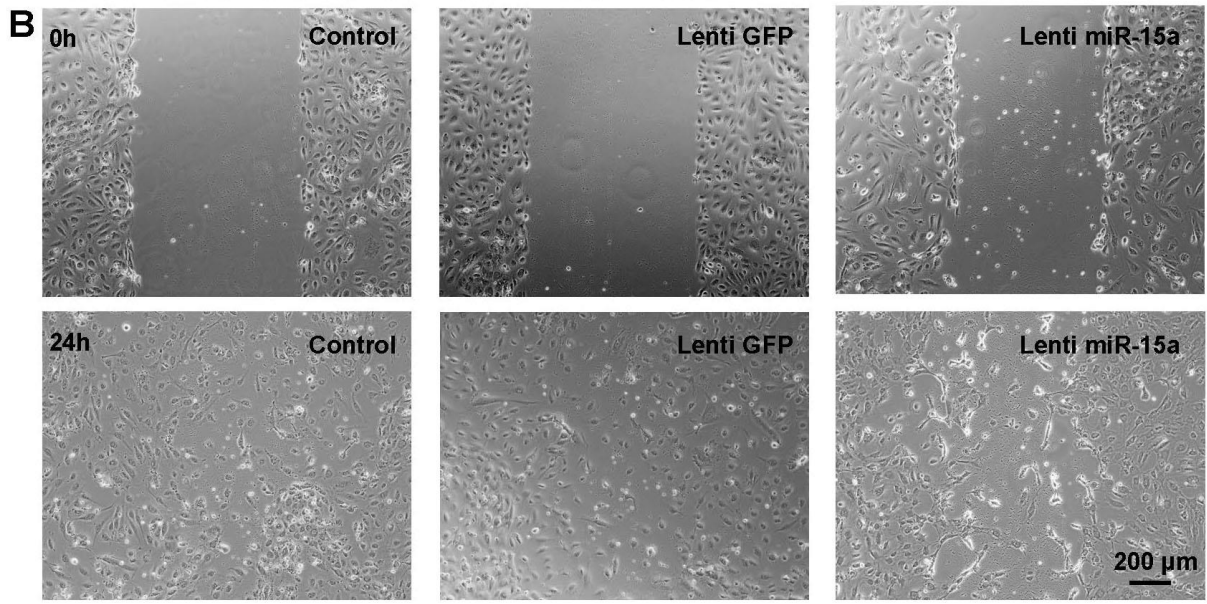
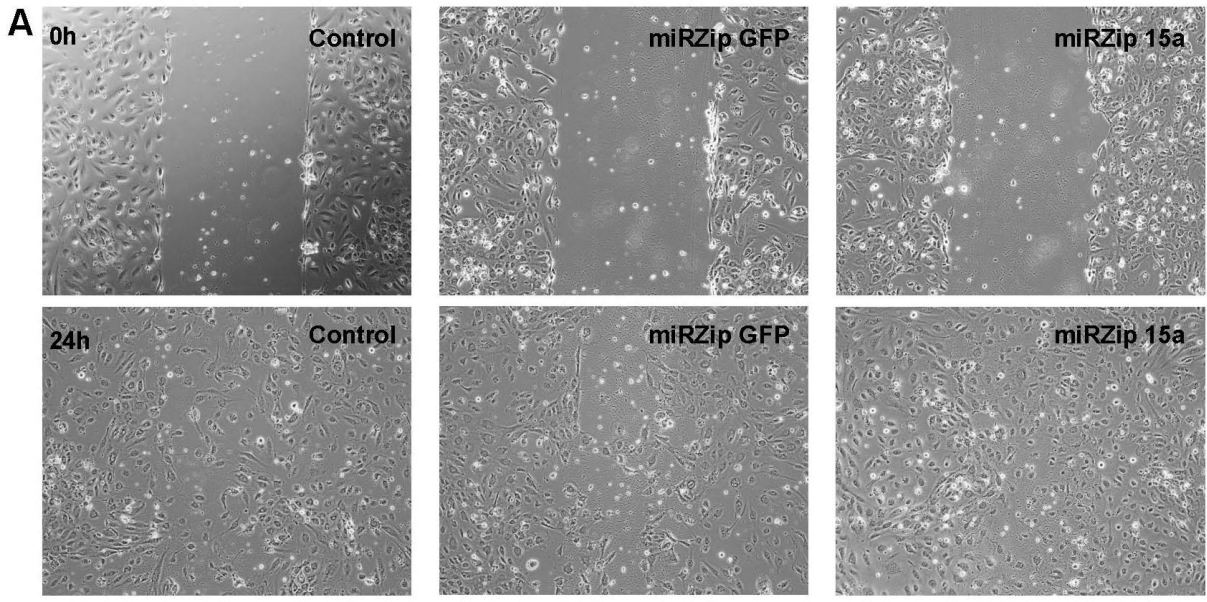
451



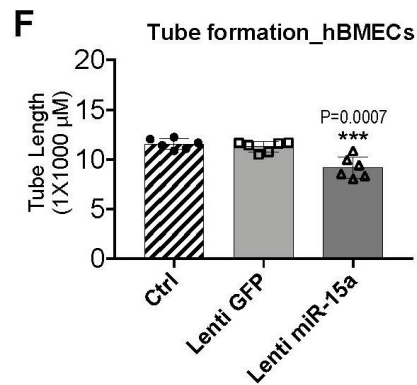
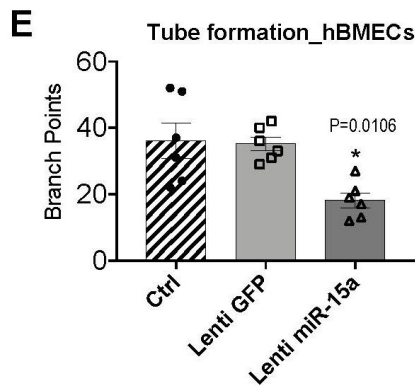
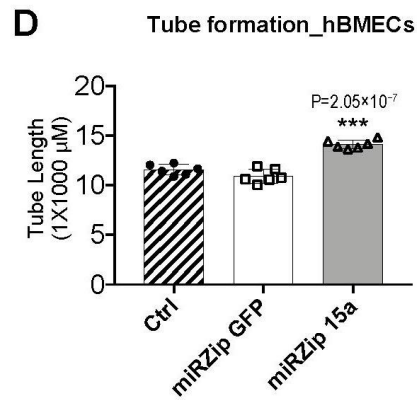
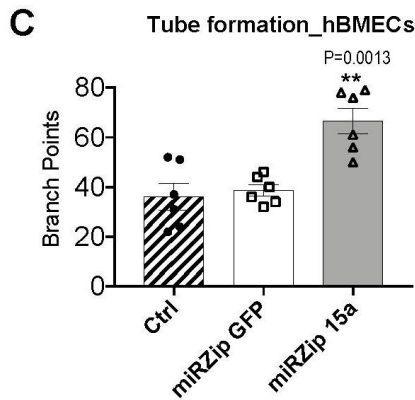
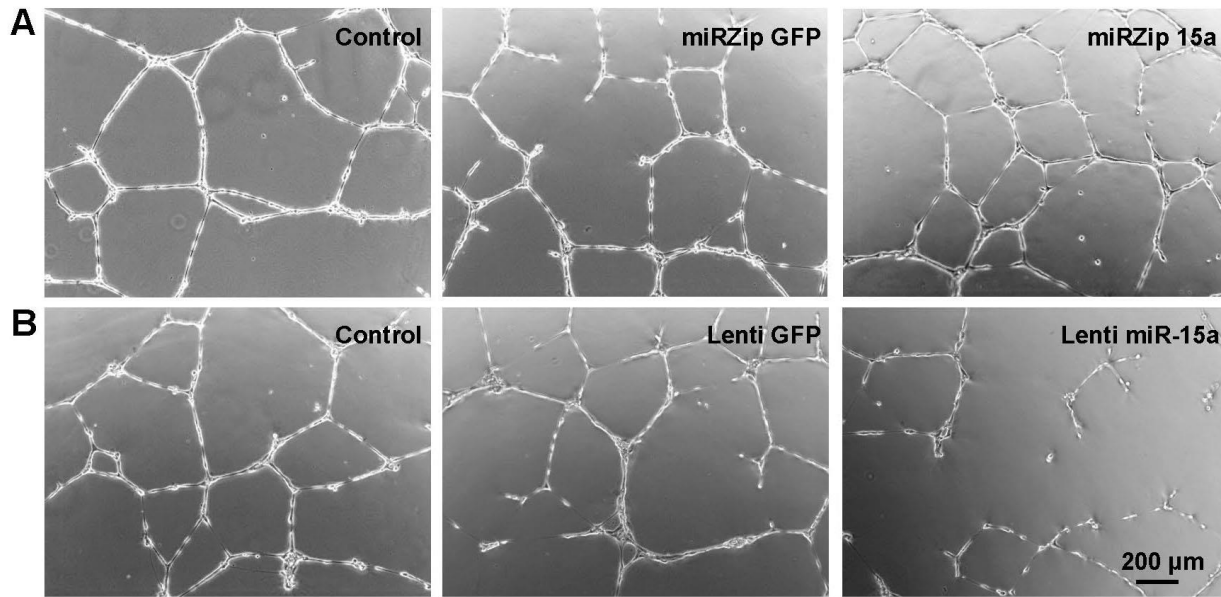
454 **Online Figure VIII. Structures of lentivirus.** *A-B*, Structures of lentivirus containing small hairpin
455 miR-15a (miRZip 15a, *B*) and its lentiviral scramble control (miRZip GFP, *A*; Cited from SBI website).
456 The inserted sequences are between H1 Promoter and 3' ΔLTR. *C-D*, Structures of lentivirus containing
457 pre-miR-15a (Lenti miR-15a, *D*) and its lentiviral GFP control (Lenti GFP, *C*; Cited from SBI website).
458 The inserted sequences are located in the multiple cloning site (MCS) between CMV and EF-1α.



460 **Online Figure IX. Lentivirus-mediated loss- or gain-of-miR-15a/16-1 function increases or**
461 **decreases cell proliferation in human brain microvascular endothelial cells (hBMECs), respectively.**
462 **A-B**, Primary hBMECs were infected with lentivirus (1-2 MOI) containing small hairpin miR-15a
463 (miRZip 15a) and its lentiviral GFP control (miRZip GFP) (**A**), or infected with pre-miR-15a (Lenti miR-
464 15a) and its lentiviral GFP control (Lenti GFP) (**B**) for 72h. **C-D**, qPCR data showed that loss-of-miR-15a
465 function in hBMECs by miRZip 15a significantly down-regulated the miR-15a expression, compared
466 with miRZip GFP group (**C**). On the contrary, gain-of-miR-15a function by Lenti miR-15a significantly
467 up-regulated the miR-15a expression, compared with Lenti GFP group (**D**). No statistically significant
468 change was observed for miR-497 expression in hBMECs treated with miRZip 15a or Lenti miR-15a,
469 compared with their lentiviral controls. Data are expressed as mean \pm SEM; n = 3/group; * p < 0.05 versus
470 lentiviral GFP groups; statistical analyses were performed by two-tailed Student's t-test. **E-F**, BrdU
471 incorporation assays showed that, loss-of-miR-15a function significantly up-regulated (**E**) while gain-of-
472 miR-15a function significantly down-regulated (**F**) cell proliferation in hBMECs, compared to their
473 lentiviral GFP groups or non-transduction controls (Ctrl). Data are expressed as mean \pm SEM; n = 4-
474 5/group; *** p < 0.001 versus lentiviral GFP groups; statistical analyses were performed by one-way
475 ANOVA followed by Tukey's multiple comparison tests.
476



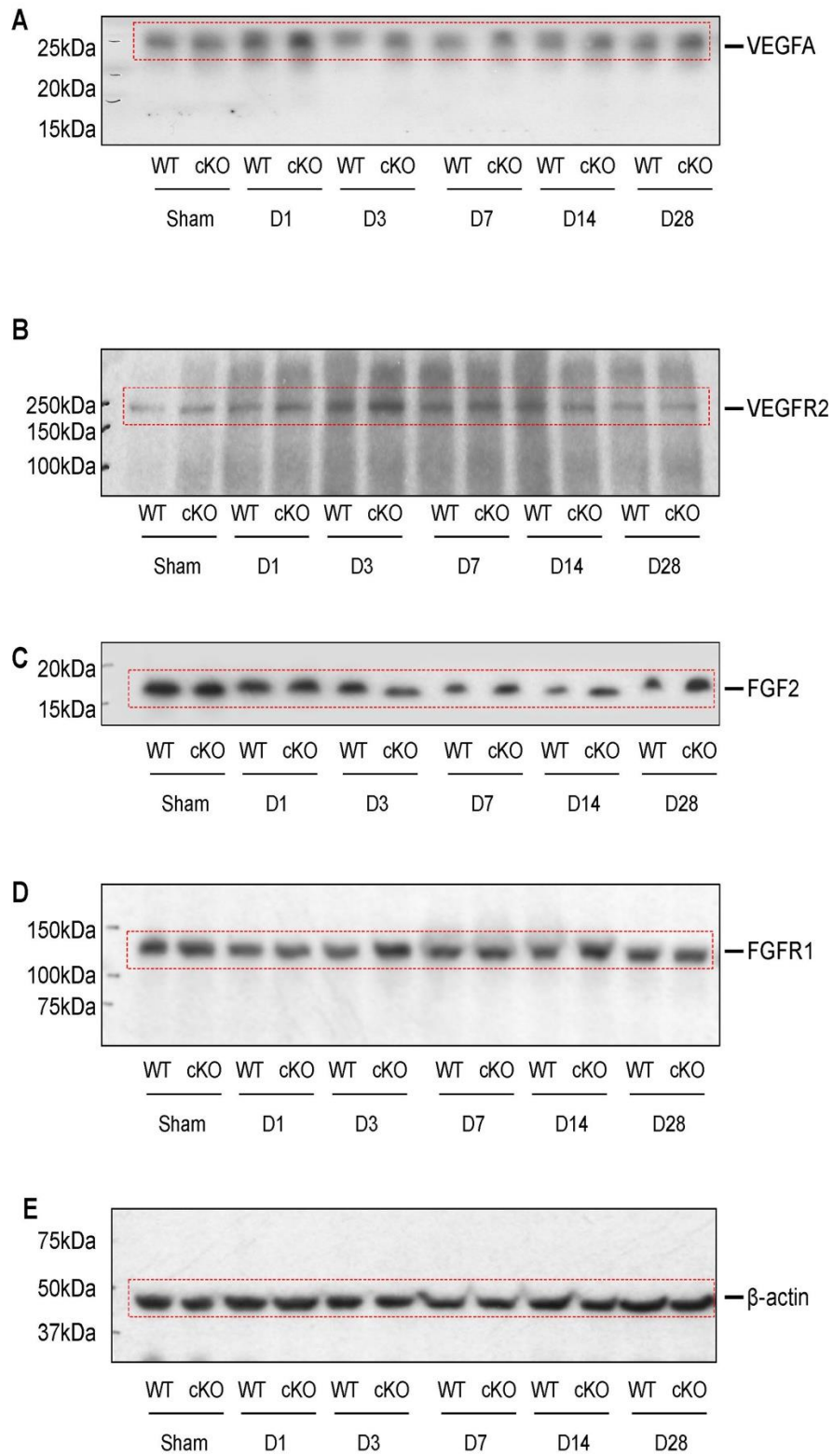
478 **Online Figure X. Lentivirus-mediated loss- or gain-of-miR-15a/16-1 function increases or decreases**
479 **endothelial migration in hBMECs, respectively.** Primary hBMECs were infected with miRZip 15a and
480 miRZip GFP or infected with Lenti miR-15a and Lenti GFP for 72h. *In vitro* scratch assay was performed
481 in hBMECs after lentiviral infections to investigate endothelial cell migration. **A,C**, Representative
482 images (**A**) and quantitative analysis (**C**) showed that loss-of-miR-15a function by miRZip 15a
483 significantly increased the endothelial cell migration in hBMECs compared to miRZip GFP group or non-
484 transduction control (Ctrl), whereas gain-of-miR-15a function (**B,D**) by Lenti miR-15a significantly
485 reversed this effect. Data are expressed as mean \pm SEM; n = 4-5/group; * $p < 0.05$, ** $p < 0.01$ versus
486 lentiviral GFP groups; statistical analyses were performed by one-way ANOVA followed by Tukey's
487 multiple comparison tests.



488

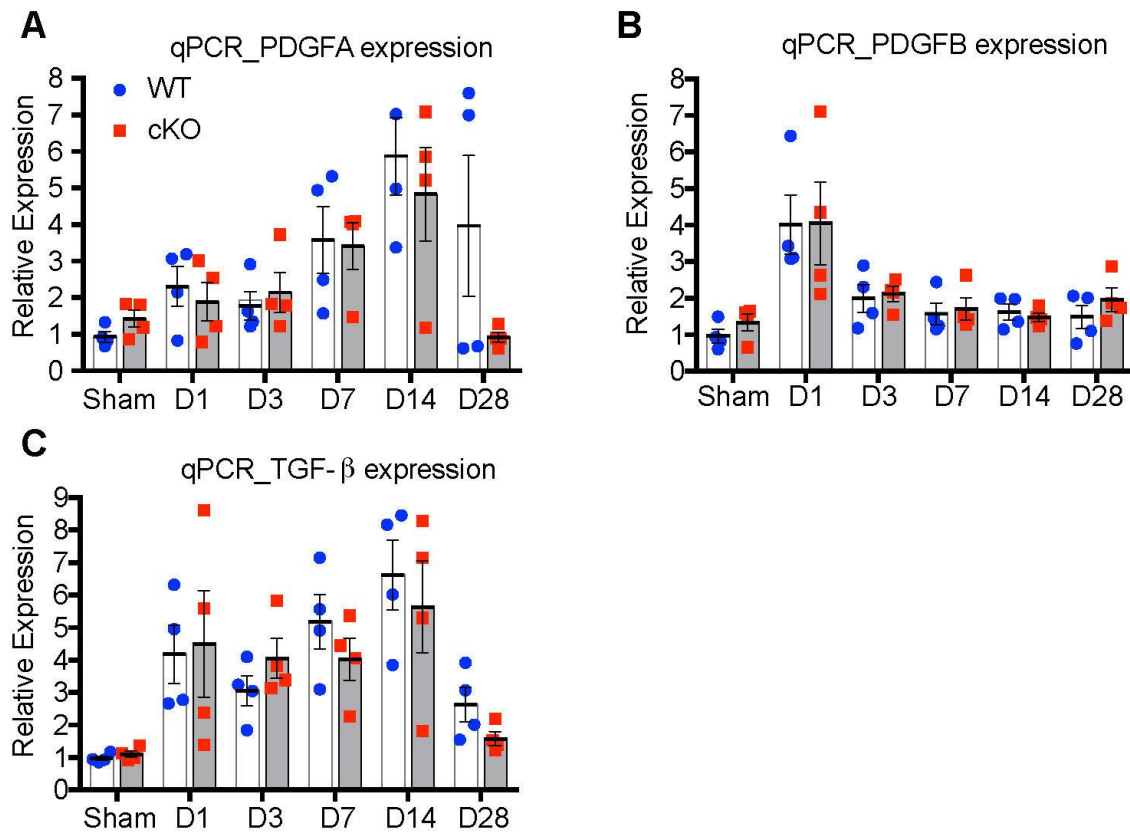
489 **Online Figure XI. Lentivirus-mediated loss- or gain-of-miR-15a/16-1 function increases or**
 490 **decreases endothelial capillary tube formation in hBMECs, respectively.** Primary hBMECs were
 491 infected with miRZip 15a and miRZip GFP, or infected with Lenti miR-15a and Lenti GFP for 72h.
 492 Capillary tube formation assay was performed in hBMECs after lentiviral infections. **A,C,D,**
 493 **Representative images (A) and quantitative analysis showed that loss-of-miR-15a function by miRZip 15a**
 494 **significantly increased tubular-like structure (A), branch points (C) and total tube length (D) . On the**

495 contrary, gain-of-miR-15a function by lentivirus dramatically reversed these effects (**B,E,F**). Data are
496 expressed as mean \pm SEM; n = 6/group; * p < 0.05, ** p < 0.01, *** p < 0.001 versus lentiviral GFP groups;
497 statistical analyses were performed by one-way ANOVA followed by Tukey's multiple comparison tests.



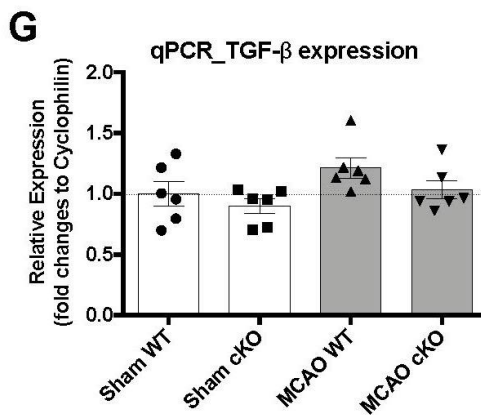
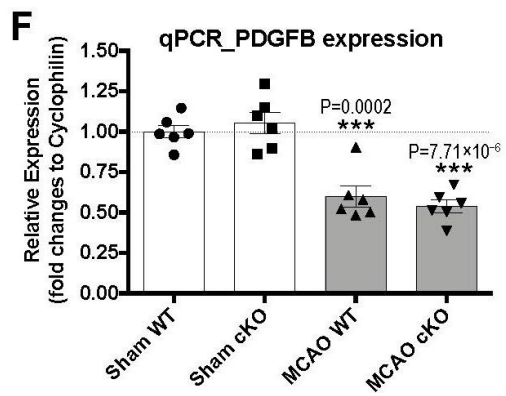
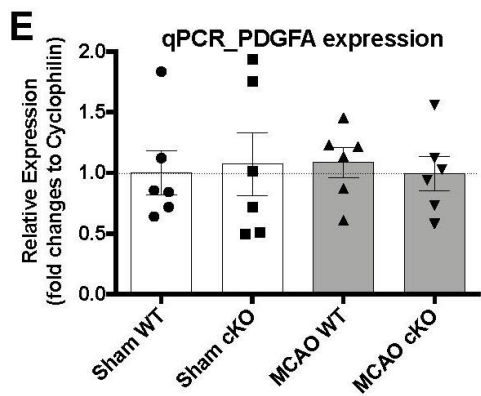
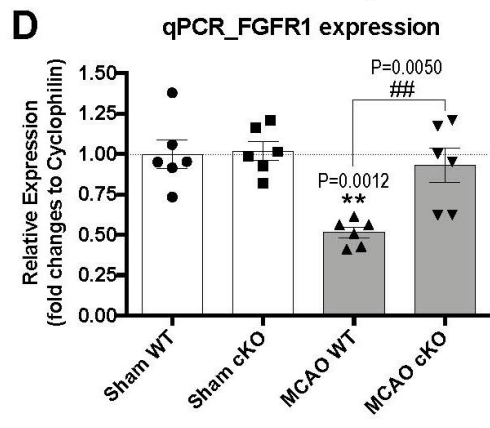
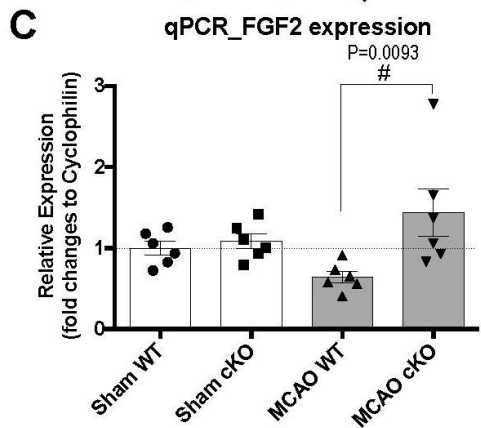
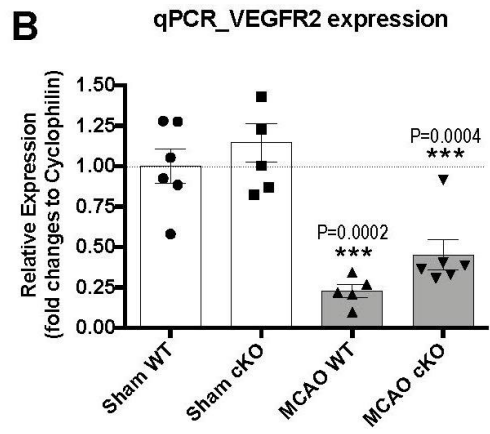
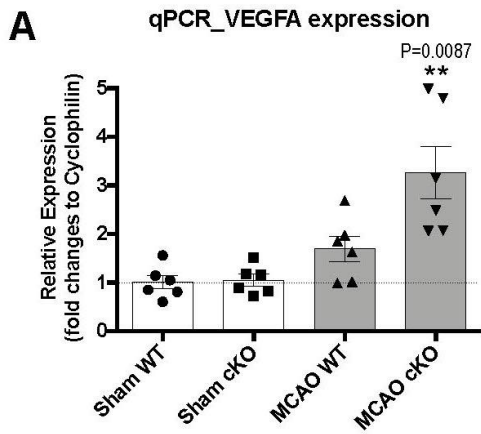
498

499 **Online Figure XII. Images of full-length blots presented in the Fig. 6.**



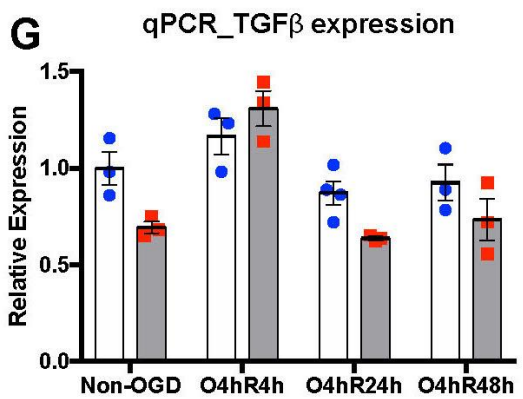
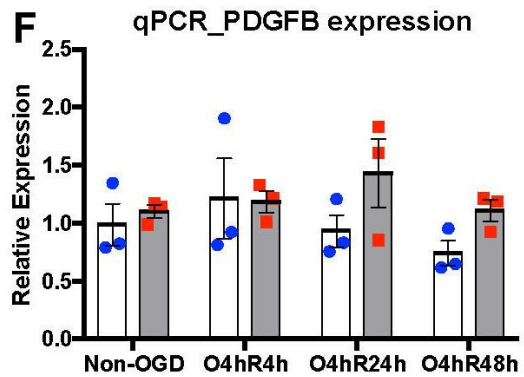
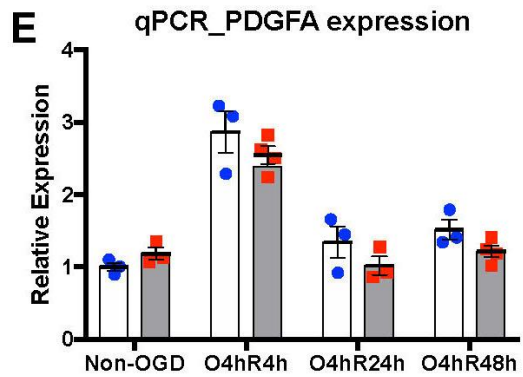
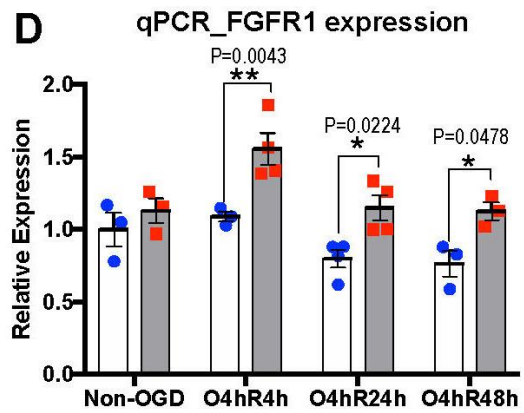
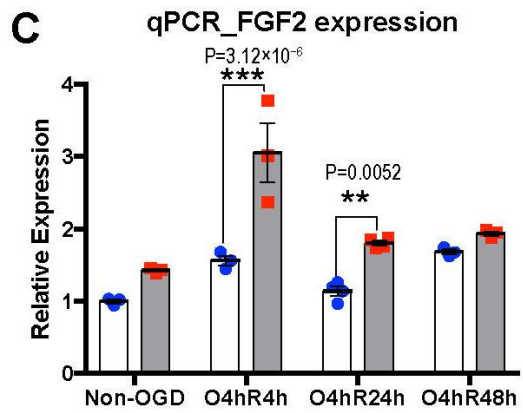
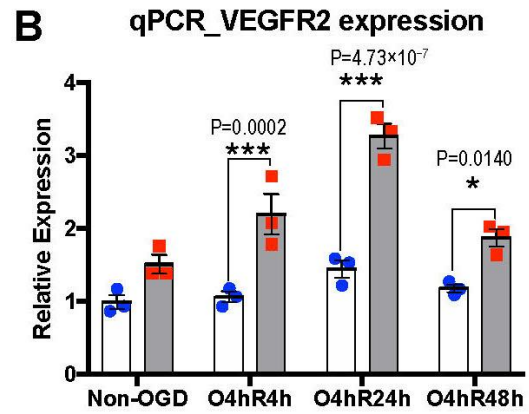
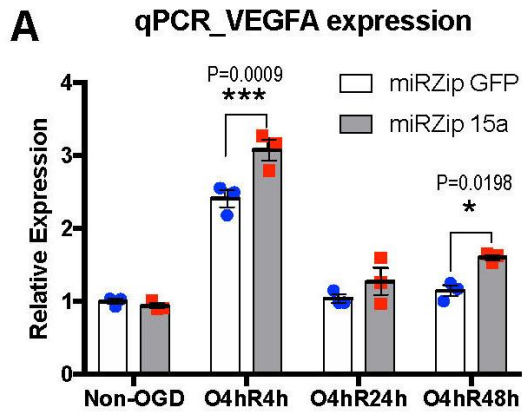
500

501 **Online Figure XIII. Endothelium-targeted miR-15a/16-1 deletion does not affect the expression of**
 502 **PDGFA, PDGF β and TGF- β in the ischemic mouse brains.** Total RNAs were extracted from the
 503 ipsilateral cortex of mouse brains at 1-28 d reperfusion after MCAO. **A-C**, qPCR data showed that the
 504 mRNA expression of PDGFA (**A**) and TGF- β (**C**) gradually increased at D1-D14 after MCAO, then
 505 decreased at D28 after MCAO for both genotypes; mRNA expression of PDGF β (**B**) increased at D1
 506 after MCAO, and then decreased and maintained at comparable level from D3 to D28 after MCAO in
 507 both genotypes. However, endothelium-targeted deletion of miR-15a/16-1 cluster (EC-miR-15a/16-1
 508 cKO) had no effects on the expression of PDGFA, PDGF β and TGF- β in ischemic mouse brains,
 509 compared with WT controls. Data are expressed as mean \pm SEM; n = 4/group; statistical analyses were
 510 performed by two-way ANOVA followed by Bonferroni's multiple comparison tests.

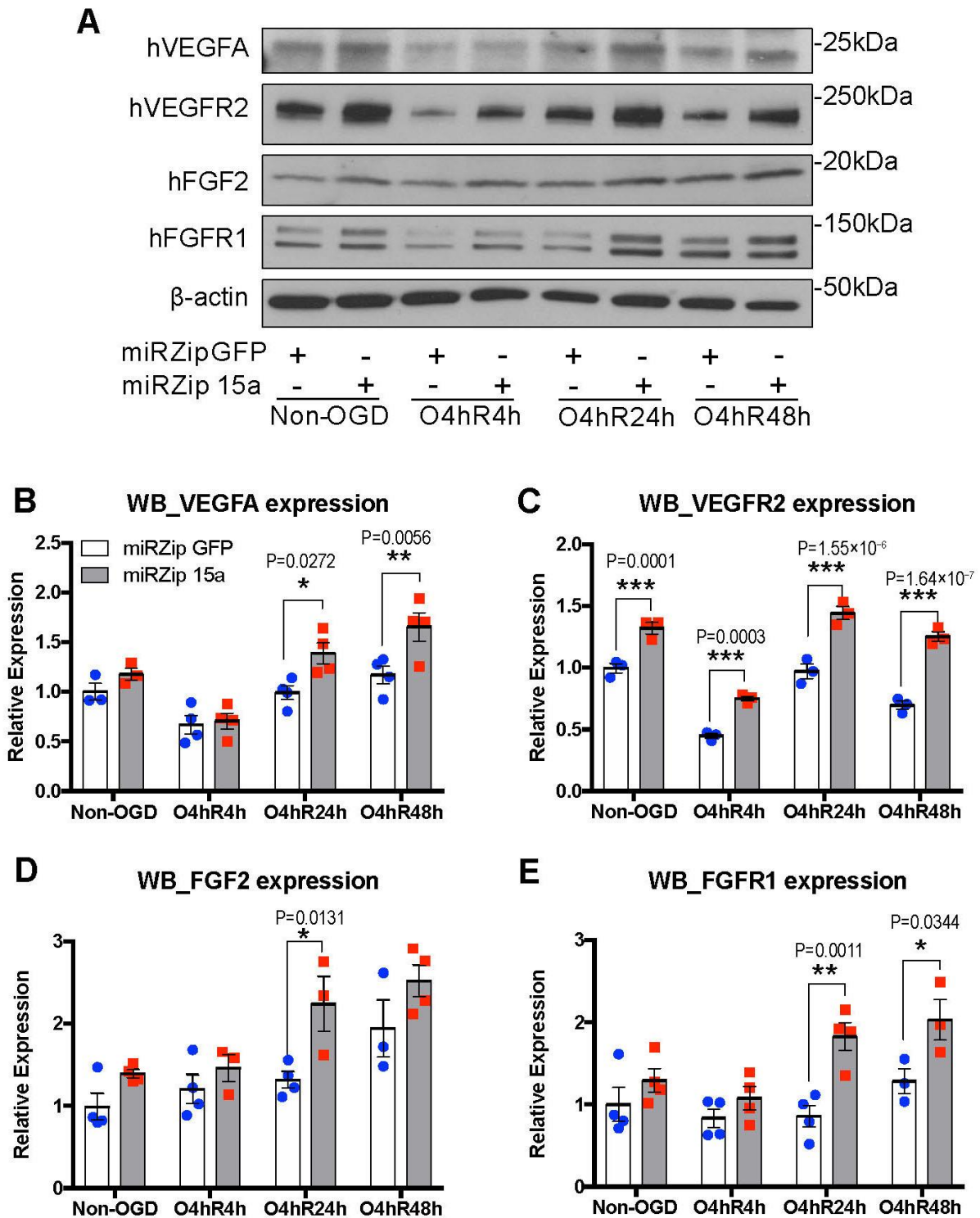


512 **Online Figure XIV. Endothelium-targeted miR-15a/16-1 deletion enhances the expression of**
513 **VEGFA, FGF2 and their receptors in the microvessels of ischemic mouse brains.** EC-miR-15a/16-1
514 cKO and WT mice were subjected to 1h MCAO followed by 14 d reperfusion. Brains were harvested and
515 microvessels were isolated from the ipsilateral hemisphere of the brain. At sham conditions, qPCR data
516 from brain microvessels showed no significant changes in the mRNA expression of indicated pro-
517 angiogenic factors between WT and EC-miR-15a/16-1 cKO groups. However, at 14 d reperfusion after
518 MCAO, qPCR data showed significantly up-regulated mRNA expression for VEGFA (**A**), FGF2 (**C**) and
519 FGFR1 (**D**), and an enhanced trend for VEGFR2 (**B**) in the brain microvessels of EC-miR-15a/16-1 cKO
520 mice compared to WT controls. No significant difference was observed for the mRNA expression of
521 PDGFA (**E**), PDGFB (**F**) and TGF- β (**G**) in the brain microvessels at the same groups 14 d after MCAO.
522 Data are expressed as mean \pm SEM; n = 6/group; ** p < 0.01, *** p < 0.0001 versus sham of each genotype;
523 # p < 0.05, ## p < 0.001 as indicated; statistical analyses were performed by one-way ANOVA followed by
524 Tukey's multiple comparison tests for **B**, **D**, **E**, **F** and **G**; statistical analyses were performed by Kruskal-
525 Wallis test followed by Dunn's multiple comparison tests for **A** and **C**.

526



528 **Online Figure XV. Knockdown of miR-15a/16-1 cluster in hBMEC cultures enhances the mRNA**
529 **expression of VEGFA, FGF2 and their receptors after OGD and reoxygenation.** Primary hBMECs
530 were infected with miRZip 15a or miRZip GFP for 72h, then cells were subjected to OGD 4h followed by
531 reoxygenation 4h (O4hR4h), 24h (O4hR24h) and 48h (O4hR48h). **A-D**, qPCR data showed that loss-of-
532 miR-15a function by miRZip15a lentivirus significantly up-regulated mRNA expressions of VEGFA (**A**),
533 VEGFR2 (**B**), FGF2 (**C**) and FGFR1 (**D**) at multiple time reoxygenation points after OGD, compared
534 with miRZip GFP groups. **E-G**, qPCR data showed that loss-of-miR-15a function by miRZip15a had no
535 significant effect on mRNA expression of PDGFA (**E**), PDGFB (**F**), TGF- β (**G**) after OGD and
536 Reoxygenation in hBMECs, compared with miRZip GFP controls. Data are expressed as mean \pm SEM; n
537 = 3-4/group; * $p < 0.05$, ** $p < 0.01$, *** $p < 0.001$ versus miRZip GFP controls at each time point; statistical
538 analyses were performed by two-way ANOVA followed by Bonferroni's multiple comparison tests.

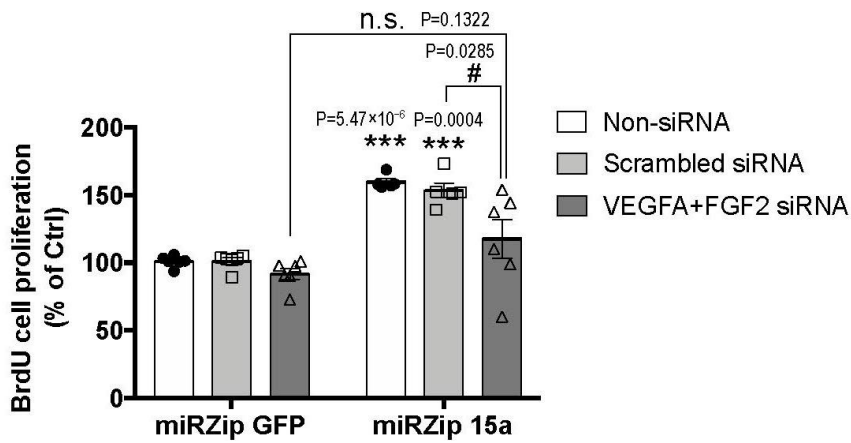


539

540 **Online Figure XVI. Knockdown of miR-15a/16-1 cluster in hBMECs cultures enhances the protein**
541 **expression of VEGFA, FGF2 and their receptors after OGD and reoxygenation.** Primary hBMECs
542 were infected with miRZip 15a or miRZip GFP for 72h, then cells were subjected to OGD 4h followed by
543 reoxygenation 4h (O4hR4h), 24h (O4hR24h) and 48h (O4hR48h). *A-E*, Representative western blotting

544 images (**A**) and quantitative analysis (**B-E**) indicated that enhanced protein levels of hVEGFA (**B**),
545 hVEGFR2 (**C**), hFGF2 (**D**) and hFGFR1 (**E**) were observed in miRZip 15a treated group at multiple time
546 points of reoxygenation after OGD, compared with miRZip GFP group. Data are expressed as mean \pm
547 SEM; n = 3-4/group; * $p < 0.05$, ** $p < 0.01$, *** $p < 0.001$ versus miRZip GFP controls at each time point;
548 statistical analyses were performed by two-way ANOVA followed by Bonferroni's multiple comparison
549 tests.
550

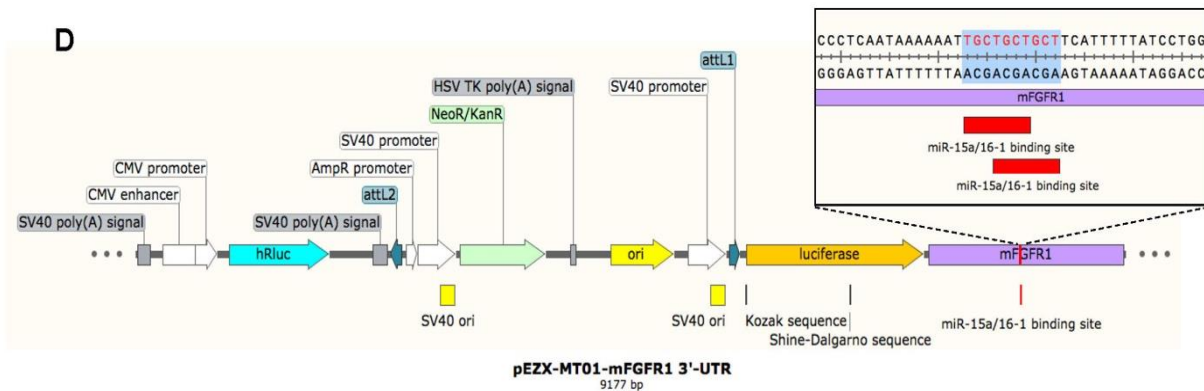
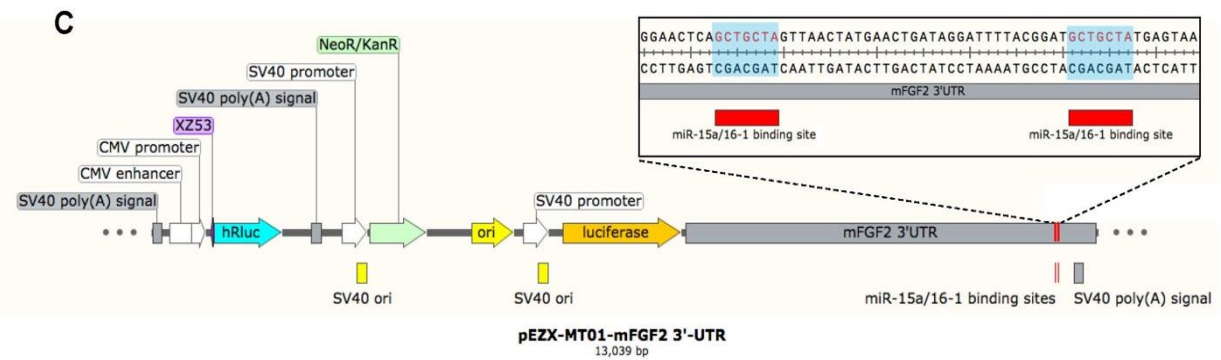
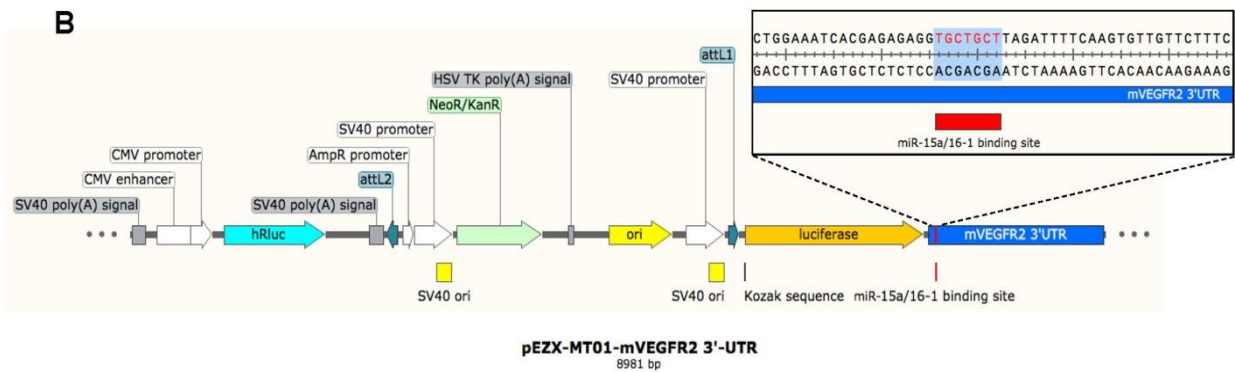
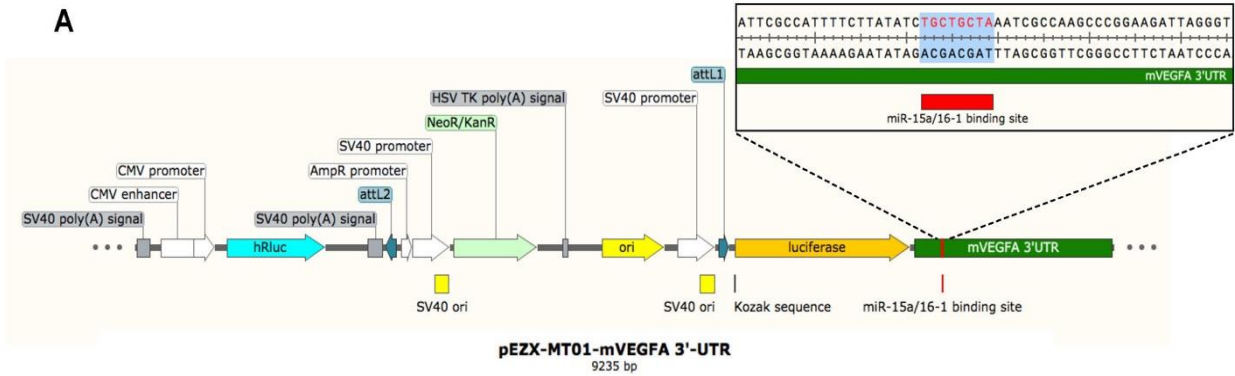
BrdU proliferation_hBMECs



551

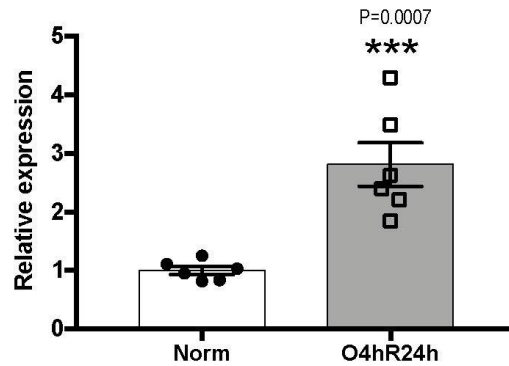
552 **Online Figure XVII. VEGFA and FGF2 signaling pathways are involved in the enhanced cell**
 553 **proliferation triggered by the loss-of-miR-15a/16-1 function in hBMECs.** Primary hBMECs were
 554 infected with lentivirus containing small hairpin miR-15a (miRZip 15a) and its lentiviral GFP control
 555 (miRZip GFP) for 72h, then cells were re-seeded in 96-well plate at 30% confluence for siRNA
 556 transfection. After cells were transfected with scrambled siRNA and VEGFA/FGF2 siRNAs, BrdU
 557 incorporation assay was performed to detect the cell proliferation. Data showed that loss-of-miR-15a
 558 function in hBMECs by miRZip 15a significantly enhanced endothelial cell proliferation compared with
 559 miRZip GFP group, when treated without siRNA (Non-siRNA) or co-transfected with scrambled siRNA.
 560 The enhanced cell proliferation triggered by the loss-of-miR-15a/16-1 function in hBMECs was almost
 561 abolished by VEGFA and FGF2 siRNAs co-treatments. Data are expressed as mean \pm SEM; n = 5-
 562 6/group. *** $p < 0.001$ versus miRZip GFP groups, ## $p < 0.01$ as indicated, n.s., no statistical significance;
 563 statistical analyses were performed by one-way ANOVA followed by Tukey's multiple comparison tests.

564



566 **Online Figure XVIII. Structures of plasmids used in the dual-luciferase reporter assay.** A
567 Firefly/Renilla dual-luciferase reporter vector (pEZX-MT01, Genecopoeia) was utilized to construct the
568 3'-UTR fragments of miR-15a/16-1 targeted genes. (A) The mouse VEGFA 3'-UTR dual-luciferase
569 reporter plasmid (pEZX-MT01-mVEGFA 3'-UTR) contains an 1862-bp fragment of the 3'-UTR
570 sequence of the mouse VEGFA mRNA, in which the putative miR-15a/16-1 binding site was shown in
571 red color. The deletion plasmid (pEZX-MT01- Δ mVEGFA 3'-UTR) carries an 1854-bp mVEGFA 3'-
572 UTR sequence in which the miR-15a/16-1 binding site was deleted (8-bp, blue colored area in the
573 magnified construct). Similarly, (B) the mouse VEGFR2 3'-UTR dual-luciferase reporter plasmid (pEZX-
574 MT01-mVEGFA 3'-UTR) contains an 1804-bp fragment of the 3'-UTR sequence of the mouse VEGFR2
575 mRNA, and the deletion plasmid (pEZX-MT01- Δ mVEGFR2 3'-UTR) carries an 1796-bp mVEGFR2 3'-
576 UTR sequence in which the miR-15a/16-1 binding site was deleted (8-bp, blue colored area in the
577 magnified construct). (C) mouse FGF2 3'-UTR dual-luciferase reporter plasmid (pEZX-MT01-mFGF2
578 3'-UTR) contains a 5666-bp fragment of the 3'-UTR sequence of the mouse FGF2 mRNA and two miR-
579 15a/16-1 binding sites. The deletion plasmid (pEZX-MT01- Δ mFGF2 3'-UTR) carries a 5626-bp mFGF2
580 3'-UTR sequence in which both of the miR-15a/16-1 binding sites were deleted (40-bp, blue-colored area
581 in the magnified construct). (D) Mouse FGFR1 3'-UTR dual-luciferase reporter plasmid (pEZX-MT01-
582 mFGFR1 3'-UTR) contains an 1804-bp fragment of the 3'-UTR sequence of the mouse FGFR1 mRNA
583 and two miR-15a/16-1 binding sites. The deletion plasmid (pEZX-MT01- Δ mFGFR1 3'-UTR) carries a
584 1794-bp mFGFR1 3'-UTR sequence in which both of the miR-15a/16-1 binding sites were deleted (10-
585 bp, blue colored area in the magnified construct).
586

Exosomal miR-15a_mBMECS



587

588 **Online Figure XIX. Oxygen and glucose deprivation stimulate mBMECs to secrete exosomal miR-**
589 **15a into the culture medium.** Primary mBMECs were grown to 90-95% confluence then subjected to 4h
590 OGD and 24h reoxygenation. Cell medium was collected, and exosomes was extracted, and then small
591 RNAs were further extracted and subjected to qPCR assays. qPCR data showed that exosomal miR-15a in
592 the culture medium was significantly elevated after 4h OGD followed by 24h Reoxygenation (O4hR24h),
593 compared to the normoxic control (Norm). Data are expressed as mean ± SEM; n = 6/group; *** $p < 0.001$
594 versus Norm; statistical analyses were performed by two-tailed Student's t-test.

595

596 **Online Table I. List of primer sequences**

Genes	Primer sequences	Annealing Temperatures	Amplicon Sizes
Cdh5-Cre Tg	forward, 5'-ACTCACACTGCCCTACCTGGAAGAAT-3'	60°C	933 bp
	reverse, 5'-AGCCCGGACCGACGATGAA-3'		
miR-15a flox	forward, 5'-TCAGTTAACCAATAAAAAGGTCAGC-3'	62°C	650 bp
	reverse, 5'-GCCTGGGTCTCACCATGTAG-3'		
mVEGF-A164	forward, 5'-AACAAAGCCAGAAAATCACTGTGA-3'	59°C	67 bp
	reverse, 5'-CGGATCTTGACAAAACAATGC-3'		
mVEGFR2 (Flk-1)	forward, 5'-TTTGGCAAATACAACCCTTCAGA-3'	59°C	133 bp
	reverse, 5'-GCAGAAGATACTGTCACCACC-3'		
mFGF	forward, 5'-GAGTTGTGTCTATCAAGGGAGTG-3'	59°C	62 bp
	reverse, 5'-CCGTCCATCTTCCTTCATAGC-3'		
mFGFR1	forward, 5'-ACTCTGCGCTGGTTGAAAAAT-3'	59°C	60 bp
	reverse, 5'-GTAGCCTCCAATTCGGTGGTC-3'		
mPDGFA	forward, 5'-GGAAGGCGTAGGGAATCAGG-3'	59°C	82 bp
	reverse, 5'-CTCACCTCACATCTGGTCGG-3'		
mPDGFB	forward, 5'-ACCAACGCCAACTTCCTG-3'	59°C	140 bp
	reverse, 5'-CGCACAATCTCAATCTTTCTCAC-3'		
mTGF-β	forward, 5'-CTATGCTAAAGAGGTCACCCG-3'	59°C	123 bp
	reverse, 5'-ACTGCTTCCCGAATGTCTG-3'		
mCyclophilin	forward, 5'-CGCTTCCCAGATGAGAACTTCA-3'	59°C	107 bp
	reverse, 5'-ACTGTGGTTATGAAGAACTGTGA-3'		
hVEGF	forward, 5'-TCCGAAACCATGAACTTTCTGC-3'	59°C	144 bp
	reverse, 5'-ATCCATGAACTTCACCACTTCGT-3'		
hVEGFR2	forward, 5'-AGCTCACAGTCCTAGAGCGT-3'	59°C	127 bp
	reverse, 5'-CACATGATCTGTGGAGGGGG-3'		
hFGF	forward, 5'-CAAGCGGCTGACTGCAAAA-3'	59°C	99 bp
	reverse, 5'-AGCTTGATGTGAGGGTCGCT-3'		
hFGFR1	forward, 5'-CCCGTAGCTCCATATTGGACA-3'	59°C	138 bp
	reverse, 5'-TTTGCCATTTTCAACCAGCG-3'		
hPDGFA	forward, 5'-CCGCCAACTTCCTGATCTG-3'	59°C	139 bp
	reverse, 5'-TTCCTGACGTATCCACCTTG-3'		
hPDGFB	forward, 5'-AGTCGGCATGAATCGCTG-3'	59°C	134 bp
	reverse, 5'-CATCAAAGGAGCGGATCGAG-3'		
hTGF-β	forward, 5'-TTGATGTCACCGGAGTTGTG-3'	59°C	130 bp
	reverse, 5'-GTAGTGAACCCGTTGATGTCC-3'		
hCyclophilin	forward, 5'-ACTCCTCATTTAGATGGGCATCA-3'	59°C	126 bp
	reverse, 5'-GAGTATCCGTACCTCCGAAA-3'		

597

ΔmVEGFA 3'-UTR	forward, 5'-GATCCGCGAGATCCTGAT-3'	58°C	374 bp
	reverse, 5'-ATCTTCCGGGCTTGGCGATTGATATAAGAAAATGGCGAAT-3'		
ΔmVEGFA 3'-UTR	forward, 5'-ATTCGCCATTTTCTTATATCAATCGCCAAGCCCGGAAGAT-3'	58°C	958 bp
	reverse, 5'-CTACTCTTTAATTAATAAATACTGTTTTAATTCTAATTAATAAG-3'		
ΔmVEGFR2 3'-UTR	forward, 5'-GATCCGCGAGATCCTGAT-3'	55°C	179 bp
	reverse, 5'-AGAACAACACTTGAAAATCTACCTCTCTCGTGATTCCAGGA-3'		
ΔmVEGFR2 3'-UTR	forward, 5'-TCCTGGAAATCACGAGAGAGGTAGATTTTCAAGTGTGTTCT-3'	55°C	1570 bp
	reverse, 5'-ACTAGTCTCGAGGGTCTCTTTAC-3'		
ΔmFGF2 3'-UTR	forward, 5'-CAAGATTTATCTAGAAATTATTAATCTAAAAATTATTT-3'	55°C	800 bp
	reverse, 5'-TCTGTACTCTACTTACTCATAGGCTGAGTTCCGTGAAGTACACA-3'		
ΔmFGF2 3'-UTR	forward, 5'-TGTGTACTTACGGAACCTCAGCCTATGAGTAAGTAGAGTACAGA-3'	55°C	1405 bp
	reverse, 5'-TAGAGTCCGGAGGCTGGATCGGTC-3'		
ΔmFGFR1 3'-UTR	forward, 5'-CGATCGCGAATTCCGTACGCTA-3'	55°C	891 bp
	reverse, 5'-ACACGCCCAGGATAAAAAATGAATTTTTTATTGAGGGAAACCT-3'		
ΔmFGFR1 3'-UTR	forward, 5'-AGGTTTCCCTCAATAAAAAATTCATTTTTATCCTGGGCGTGT-3'	55°C	976 bp
	reverse, 5'-ACTAGTCTCGAGGTAGACCTGAG-3'		

598

599 Primers of Cdh5-Cre Tg were used in genotyping to identify the VE-Cadherin-Cre-recombinase
600 transgenic mouse, and primers of miR-15a flox were used in genotyping to identify the miR-15a/16-1
601 floxed mouse. Primers of mouse (m) or human (h) VEGFA, VEGFR2, FGF2, FGFR1, PDGFA, PDGFB,
602 TGF-β and cyclophilin were used in qPCR to detect their relative mRNA expressions. Primers for
603 ΔmVEGFA 3'-UTR, ΔmVEGFR2 3'-UTR, ΔmFGF2 3'-UTR and ΔmFGFR1 3'-UTR were used to
604 generate the mouse VEGFA, VEGFR2, FGF2 and FGFR1 3'-UTR plasmids with deletions of miR-
605 15a/16-1 binding sites, respectively, for dual-luciferase reporter assay. Base pair (bp).

606

607 **Online Table II. List of primary antibodies**

Antibody	Host species	Dilution used	Company	Ref #
mouse CD31	Rat	1: 200	BD Pharmingen (San Diego, CA, USA)	553370
mouse microtubule-associated protein 2 (MAP2)	Rabbit	1: 500	EMD Millipore (Burlington, MA, USA)	AB5622
5-bromo-2'-deoxyuridine (BrdU)	mouse	1: 200	BD Pharmingen	555627
mouse VEGFA	Rabbit	1: 500	Abcam (Cambridge, MA, USA)	ab51745
mouse/human VEGFA	Rabbit	1: 500	Abcam	ab46154
mouse/human VEGFR2	Rabbit	1: 500	Cell Signaling (Beverly, MA, USA)	2479L
mouse/human FGF2	Rabbit	1: 800	Sigma-Aldrich (St.Louis, MO, USA)	SAB2108135
mouse/human FGFR1	Rabbit	1: 1000	Cell Signaling	9740S
β-actin	Mouse	1: 2000	Sigma-Aldrich	A5441

608

609